Content Promotion for Online Content Platforms with Diffusion Effect

Yunduan Lin[1], Mengxin Wang[2], Zuo-Jun Max Shen[2], Heng Zhang[3], Renyu Zhang[4]

[1] Civil and Environmental Engineering Department, University of California, Berkeley

[2] Industrial Engineering and Operations Research Department, University of California, Berkeley

[3]W. P. Carey School of Business, Arizona State University

[4]CUHK Business School, The Chinese University of Hong Kong

yunduan_lin@berkeley.edu,mengxin_wang@berkeley.edu,maxshen@berkeley.edu,
hengzhang24@asu.edu,philipzhang@cuhk.edu.hk

Problem Definition: Content promotion policies are playing an increasingly important role in improving content consumption and user engagement for online content platforms. However, a frequently used promotion policy generally neglects employing the diffusion effect within a crowd of users. In this paper, we study the candidate generation and promotion optimization (CGP) problem for online content through incorporating the diffusion effect. We also investigate ways to use the content adoption data to estimate the diffusion effect and to optimize the content promotion decision. **Methodology:** We propose a diffusion model for online content that captures platform promotions. Using the diffusion model to characterize the diffusion process, the CGP problem is formulated as a mixed-integer program, which turns out to be NP-hard and highly nonlinear. Furthermore, taking advantage of the rich data available from the online platforms, we propose double ordinary least squares (D-OLS) estimators for diffusion coefficients. **Results:** We prove the submodularity of the objective function for the CGP problem, which yields an efficient $(1-1/e)$-approximation greedy solution. We show that the D-OLS estimators are consistent and more efficient (i.e., with smaller asymptotic variances) than the traditional OLS estimators. Numerical results based on real data from a large-scale video sharing platform show that our diffusion model effectively characterizes the adoption process of online content. In addition, our proposed content promotion policy can increase the total adoption by 22.48% when benchmarked against the policy actually implemented on the platform. **Managerial Implications:** We not only highlight the essential differences between the diffusion of online content and that of physical products but also provide actionable insights for online content platforms to substantially improve the effectiveness of a content promotion policy by leveraging our diffusion model.

Key words: Online Content, Diffusion Modelling, Promotion Optimization, Approximation Algorithms

1. Introduction

In recent years, online content platforms such as Tiktok and Instagram have achieved considerable success in parallel with the proliferation of social media. Online content comes in various forms, including reviews, blogs and videos. Analogous to traditional online retailers, an online content platform also regards the content as its virtual product to attract users. However, there are several features unique to online *content* platforms. (i) *Platform objective*: While retail platforms aim to maximize the revenue obtained from selling products, content platforms aim to maximize the engagement of users and the impact of their content. For example, the total number of content clicks, which we adopt as the key metric in our work, is widely recognized as a vital metric for platform operations (Su and Khoshgoftaar 2009). (ii) *Scale*: The amount of content is orders of magnitude larger than the number of products on an online retail platform. New content is generated at a significantly faster speed than new products are introduced on an online retail platform. For instance, Amazon sells 12 million products in total (AMZScout 2021), while YouTube has more than 500 hours of videos (YouTube 2021) uploaded per minute, with an average video length of 11.7 minutes (Statista 2021). A rough estimate implies millions of new videos are uploaded every day. (iii) *User consumption behavior*: Instead of directly searching for a particular product of interest as they would in an e-commerce setting, online content platform users rely heavily on platform promotions and/or friends sharing content on a social network as ways to overcome information overload (Anandhan et al. 2018).

More specifically, on the one hand, the platform is able to promote content to users intending to receive direct clicks. On the other hand, users are encouraged to share the content they find interesting with others in social media communities, which results in content diffusion on the platform. Diffusion enables more users to see and click the content without a direct platform promotion. Diffusion indeed significantly boosts user engagement for an online content platform. As a concrete example, from the data of a large-scale video sharing platform we work with, we notice that 27.73% of the clicks come from the diffusion effect.

Example 1 (The diffusion of one piece of content). Some articles that announce breaking news or tell good stories might go viral on the platform when many users cascadingly repost them. For instance, in 2020, a local news story about two missing children in Florida netted almost 3.5 million shares on Facebook (FOX32 2020).

Example 2 (The diffusion of a trend). Some content that is of the same category, of similar nature, or with homogeneous topics is usually associated with trending hashtags and/or headlines. As more users are aware of, and engaged in this trend, the related content will also become popular. For instance, the hashtag *#squidgame* has garnered 72.4 billion views on TikTok (TikTok 2021). Numerous TikTok users became part of the trend; an enormous amount of content, including reenactments of the game, makeup looks and Halloween costumes inspired by the TV show "Squid Game", was produced and viewed on TikTok.

The online content platform's business model prompts the following research question:

> *How can a content promotion strategy be designed that selects a small subset of content from the enormous content corpus to display to users, such that the total number of content clicks is maximized?*

Previous literature often focuses on maximizing the number of clicks directly from a promotion, hence ignoring the diffusion effect. It suggests promoting content with a high historical click-through rate in the hope of attracting clicks directly (Feng et al. 2007, Liu et al. 2010). However, as this type of promotion strategy focuses on content already demonstrated to be successful, it tends to promote only a small portion of content that is already consumed by a large proportion of users—a "rich get richer" type of strategy. Moreover, ignoring the diffusion effect may reduce recommendation efficiency, hurt diversity, and diminish the long-term payoffs (Vahabi et al. 2015). This is because the diffusion effect itself can effectively accelerate the spread of the content with high historical click numbers across the social network without being directly promoted by the platform. In contrast, content with a high potential to spread but limited historical exposure to users may be ignored and quickly purged from the system. To the best of our knowledge, these trade-offs are largely unexplored in the literature.

In this study, we aim to fill this gap by developing a diffusion-based promotion strategy for online content platforms. A machine-learning-based promotion strategy in practice typically is comprised of two stages: candidate generation and promotion optimization (Davidson et al. 2010, Covington et al. 2016). In the candidate generation stage, a small subset of content is chosen from a universal corpus of content. In the promotion optimization stage, the platform allocates the limited promotion bandwidth to each candidate content. To emphasize computational efficiency, the two-stage procedure winnows down a large volume of content and steers the focus in the resource allocation stage to a small portion of content that can potentially generate high rewards. With an eye on the implementability of our proposed methods, we follow this existing two-stage framework but we also emphasize two distinct features that vary from the existing machine-learning-based strategies. First, we take into account the diffusion effect. Second, we note that the candidate set selection would naturally impact the optimal allocation of user attention to the content. We therefore carefully treat these two stages as a whole to maximize the total number of clicks, as opposed to considering them as separate machine learning tasks as in the previous literature.

To characterize the diffusion process of online content, we propose the online Bass diffusion model (OBM) adapted from the well-known Bass diffusion model (BDM, Bass 1969). Specifically, we inherit the notion of *innovative* and *imitative* effects from BDM. In the context of online content platforms, we interpret them as two sources of user consumption and clicks, i.e., platform promotion and user sharing, respectively. As we will show in this paper, the BDM fits the diffusion process of online content poorly because it overlooks a platform's influence on diffusion and the users' time-decaying willingness to share content. We introduce the OBM with both effects explicitly captured. We empirically demonstrate that the OBM is able to provide an excellent fit for the diffusion process on a real-world online content platform. Furthermore, it allows us to integrate the candidate generation and promotion optimization (CGP) problems into a succinct mixed-integer program and obtain high-quality approximate solutions with performance guarantees. Additionally, leveraging the high-granularity data commonly available on online content platforms, we design an estimation method of both *innovative* and *imitative* coefficients for the OBM. Counterfactual analyses based on real data from a large-scale online content platform demonstrate the effectiveness of our modeling framework, optimization algorithm and estimation strategy. In short, based on the OBM, we offer a set of complete solution techniques for the online content promotion problem and demonstrate its effectiveness through extensive numerical experiments.

1.1. Contribution and Organization

We detail our contribution as follows.

- **A diffusion model for online content.** We propose to model the diffusion of online content using OBM, which extends the BDM by incorporating the platform promotion intensity. From the theoretical side, OBM explicitly characterizes the relationship between the platform's promotion decisions and the diffusion process. It provides a concise way to optimize the platforms' decisions. From the practical side, we show that the OBM is well suited for a real adoption curve from a large-scale real-world dataset. We test the prediction accuracy of the OBM relative to the classical BDM. This comparison shows that OBM improves the weighted average mean absolute percentage error (MAPE) by 107.05% to 22.76% of the number of new adopters among all the content categories
- **Formulation and algorithmic design for the CGP problem.** Using the OBM to characterize the diffusion process, we formulate the CGP problem as a mixed-integer optimization problem in which we jointly determine both the set of content to promote to users and the promotion probabilities. Although the CGP problem has nonlinear constraints and is provably NP-hard, we show that the subproblem of CGP when the candidate set is fixed has an objective function that is separable, strictly monotone and concave in the promotion probabilities. We demonstrate that we can efficiently solve the subproblem with a subroutine based on the Karush–Kuhn–Tucker (KKT) conditions. By analyzing the structural properties of the subproblem, we establish the submodularity of the candidate set selection problem, which at a glance seems intractable, as it does not admit an explicit expression. Combined, we are able to provide a $(1-1/e)$-approximation algorithm for the CGP problem following the well-known greedy algorithm for submodular problems (Nemhauser et al. 1978). Furthermore, we notice that the subproblem can be further simplified when embedded in the greedy framework by leveraging the structural properties of the CGP problem. Therefore, we can cut the running time for the approximation algorithm from $\mathcal{O}(|\mathcal{V}|K^3)$ to $\mathcal{O}(|\mathcal{V}|K^2)$, where $|\mathcal{V}|$ is the total amount of content and K is the capacity of the promotion candidate set. Numerical experiments demonstrate the computational accuracy and efficiency of our proposed algorithm.

- **A new estimation approach based on OBM.** Standard estimation techniques for BDM may not work well for OBM due to the severe collinearities and autocorrelations inherent in the problem. We propose a double ordinary least squares (D-OLS) method for OBM parameter estimation that utilizes the platform's ability to keep track of the innovators and imitators throughout the diffusion process. We show that the D-OLS estimators are asymptotically consistent and achieve much smaller asymptotic variances than the OLS estimators.
- **Extensive numerical experiments with real datasets.** We evaluate our models and algorithms using a large-scale real-world dataset from an online video sharing platform. Our observations are threefold. First, we showcase the real-world diffusion effect of online content. In general, the value of the innovative coefficient for online content is significantly larger than that of traditional BDM, which highlights the importance of promotion decisions for online content platforms. We further find that the innovative and imitative effects across different content categories are highly heterogeneous. Different content exhibits diverse adoption patterns. Additionally, the innovative and imitative coefficients for the same content category are slightly negatively correlated. Therefore, focusing only on adoptions from direct promotions can potentially miss out on the opportunities of enjoying the benefit of diffusion. These facts demonstrate the trade-off between innovative and imitative rewards and corroborate the nontriviality of the CGP problem. Second, we show that our proposed adaptive greedy algorithm achieves a substantial improvement from the benchmarks that only consider historical popularity, direct attractiveness, or no diffusion effect. An improvement of at least 22.48% is achieved. Third, we find that the length of the promotion horizon and the associated frequency of resolving the CGP problem are of great importance to balance the trade-off between diffusion rewards and policy flexibilities. Considering a longer time period for the CGP problem allows the platform to take more imitative effects into consideration when deciding promotion policies. However, the resulting updates on promotion decisions becomes less frequent, which can diminish the total reward. Our experimental results illustrate such a trade-off and verify that in reality the promotion strategy overlooks the diffusion effect. Furthermore, the results show that the optimal promotion horizon length increases with the promotion capacity of the platform.

The remainder of the paper is structured as follows: In Section 2, we review the related literature. In Section 3, we discuss the OBM. In Section 4, we formulate the CGP problem and propose an adaptive greedy algorithm for solving it. In Section 5, we discuss the estimation issues for the OBM. Section 6 presents our numerical studies based on real-world data, followed by concluding statements in Section 7.

2. Literature Review

As we discussed earlier in the introduction, promotion and diffusion are two main sources of rewards for the online content platform. Therefore, we focus our literature review on promotion policies and diffusion effect studies. From the perspective of the platform, its goal is to provide users with content that maximizes its total reward. An active stream of literature is about recommender systems (RSs), which focuses on investigating the connections between users and content. Various recommendation algorithms (Resnick et al. 1994, Kitts et al. 2000, Covington et al. 2016) have been proposed to evaluate the probability that users are likely to click a particular item. However, the click-through rate only characterizes the immediate interactions between the platform and the users. Some recent work (Azaria et al. 2013, Lu et al. 2014, Besbes et al. 2016) demonstrated that maximizing the immediate item relevancy does not align with utility maximization in RSs. The reasons are various, and one of the most important issues is the consequent diffusion within the underlying social network. Although there is a rich line of work (Liu and Aberer 2013, Ma et al. 2015) exploiting social networks for more contextual information, quite a few of the studies incorporate the diffusion effect. Vahabi et al. (2015) is the first to mention that the availability of social networks can empower the utility maximization of RSs. In other words, not only do directly targeted users contribute to the total adoption but also the users who are influenced by their accounts. They proposed a social-diffusion-aware RS that can efficiently use recommendation slots and enhance the overall performance. Our work substantially differs from Vahabi et al. (2015). They utilized a personalized recommendation scheme with a hard constraint that no neighbors receive the same content. Thus, the potential diffusion may increase the total reward. We instead characterize the entire diffusion trend over the population and attempt to find an optimal promotion policy.

We remark that our work does not emphasize mining the relationship between users and content or personalized recommendations from a machine learning perspective, as in the literature discussed above. Typically, these works separately consider the content recommendation for each user. Rather, we take a holistic approach and study the problem from an operations perspective. Our intent is to maximize the total clicks by modeling the whole process as a diffusion problem on a social network and generate high-quality solutions using combinatorial optimization techniques.

To understand how the interaction between users affects their adoption, many diffusion models have been proposed in the marketing and information systems literature. Pioneered by Bass (1969), the BDM has become the most widely used diffusion model for new products, capturing the adoption trend with the use of parsimonious differential equations. A sequence of work (Easingwood et al. 1983, Horsky and Simon 1983, Norton and Bass 1987) extends BDM by incorporating different dynamics, such as nonuniform influence and multiple generations. BDM has achieved tremendous success in predicting the adoption level of a variety of products, including consumer durable goods, medical innovations (Sultan et al. 1990) and information technology innovations (Teng et al. 2002). Bass et al. (1994) then developed a generalization of BDM that introduces decision variables such as price or advertising into the model. This generalization sheds light on the marketing strategy with diffusion as a consideration. Although BDM has a long history, it consistently attracts researcher's attention and is often applied in new contexts (Jiang and Jain 2012, Agrawal et al. 2021). Our diffusion model is also an extension of BDM through introduction of the promotion decision. It follows the promotion logistics of online content platforms and explains the underlying diffusion behavior.

BDM and all the aforementioned models consider the global network effect, where the user behavior depends on the overall adoption level of the entire market. Although it does not explicitly embed the structure of social networks, it has the advantage of being simple and efficient to use in prescriptive optimization problems. In contrast, the local network effect is also considered in some other works, with a specific formation of the user network. Each individual is only influenced by a local neighborhood in the network. This kind of diffusion will result in extreme adoption dynamics as each user has idiosyncratic behaviors. The independent cascade (IC) model (Goldenberg et al. 2001) and linear threshold (LT) model (Granovetter 1978, Schelling 2006) are two of the most fundamental models with local network effects. Kempe et al. (2003) modeled the influence maximization (IM) problem as an algorithmic problem with the goal of finding the best subset of seed users that could trigger the maximum adoption. Arora et al. (2017) and Li et al. (2018) provided a comprehensive experimental study and survey on IM, respectively. For other applications, we refer readers to review papers (Kiesling et al. 2012, Zhang and Vorobeychik 2019). The diffusion process of the local network effect model cannot be easily quantifiable through a simple formula; hence, the characterization of the market relies heavily on simulation techniques, and the subsequent optimization problem is time-consuming to solve. Furthermore, the local network structure among users may not be observable or subject to change, which increases the implementation difficulties. Owing to such limitations, we focus on the global diffusion effect in this work.

Another branch of study that is related to our work is revenue management for online retailers. In practice, hundreds of thousands of pieces of content compete for limited promotion opportunities. Therefore, we need to consider candidate generation and promotion optimization jointly for all content. Although users exhibit different choice behaviors, the candidate selection and promotion optimization has some similarities to the assortment planning and pricing problem. Golrezaei et al. (2020), Chen and Shi (2019) presented the inventory and pricing strategies for different strategic customers that have seemingly similar user behavior on an online content platform. Moreover, some recent works also consider the network effect in traditional operations management problems. Hu et al. (2016) considered the case where purchase decisions can be influenced by earlier purchases.

(Du et al. 2016, Wang and Wang 2017) proposed a variant of the multinomial logit (MNL) model incorporating the network effect in an assortment optimization problem. Follow-up work (Nosrat et al. 2021, Chen and Chen 2021) also involved different choice models. These studies rely on the problem structure of traditional assortment/pricing problems and achieve efficient algorithms. This motivates us to consider the problem of online content platforms.

3. Online Bass Diffusion Model (OBM)

In this section, we formally introduce the online Bass diffusion model. We start by providing a motivating observation from a real-world dataset and then describe the details of the OBM.

3.1. Background and Motivation from a Large-Scale Video-Sharing Platform

For completeness of discussion, we give a brief overview of the Bass diffusion model (BDM) for the readers. In general, BDM describes the process of how new products are adopted in a population. The basic premise of the BDM is that adopters can be classified into *innovators* and *imitators*. Innovators refer to the individuals who decide to adopt the product independently, and imitators refer to the adopters that are influenced by others. However, due to the limitation of data acquisition techniques, innovators and imitators are not identifiable in the traditional market.

The diffusion unfolds in discrete steps. More specifically, in a discrete-time horizon $t = 1, 2..., L$, the BDM models the number of new adopters at time t as

$$a_t = \left(p + \frac{q}{m} A_{t-1}\right)(m - A_{t-1}) \quad \forall t = 1, ..., L,$$

where $A_{t-1} = \sum_{\tau=1}^{t-1} a_\tau$ is the number of cumulative adopters until time period $t-1$, m is the market size, and p and q are the innovative coefficient and imitative coefficient, respectively. In particular, $(p + q/m \cdot A_{t-1})$ represents the probability that an individual adopts the item at period t given that she did not adopt it in periods 1,2..., $t-1$. This suggests that the probability that a user makes an adoption at time t is influenced by two forces: the innovative effect p and the imitative effect $q/m \cdot A_{t-1}$, which is proportional to the number of users that have already adopted the item. To ensure the well-definedness of the discrete time BDM, it is commonly assumed that $p \geq 0$, $q \geq 0$, and $p + q \leq 1$. If historical adoption data are available, p and q can be estimated via the standard least-squares estimation (see Section 2.6.3 of Snyder and Shen (2019)).

It seems conceptually straightforward to apply the BDM to online content platforms. In this case, we let the market size m be the total number of users on the platform. We use the terms "click" and "adoption" interchangeably. Furthermore, we view adopters who received the promotion from the platform as innovators.

When the user adopts from her friend sharing the content without being targeted by a promotion, we refer to her as an imitator. To test if the BDM works as desired, we investigate the video click data from a large-scale video-sharing platform and fit the BDM model using the standard least-squares estimation with these data. For more information about the platform and the data, please refer to Section 6.1. For details of the estimation procedure, please refer to Appendix C.1 The high-granularity data from this platform helps us to differentiate between the two types of adopters by tracing the promotion history. This can provide us with more insights.

In particular, we focus on a single video that exhibits the typical pattern of the online diffusion process. Figure 1a shows how the new adopter curve of the BDM drastically deviates from the true trajectory. Note that we fit the BDM model using the first 50 time periods, and it naturally predicts a steady growth of new adopters in the near future, whereas the real data, in fact, shows a quick drop of the actual adopter count. To further understand the driving force here, we take a closer look at the number of innovators and imitators separately and observe that their growth patterns are not captured by BDM (Figure 1b and Figure 1c).

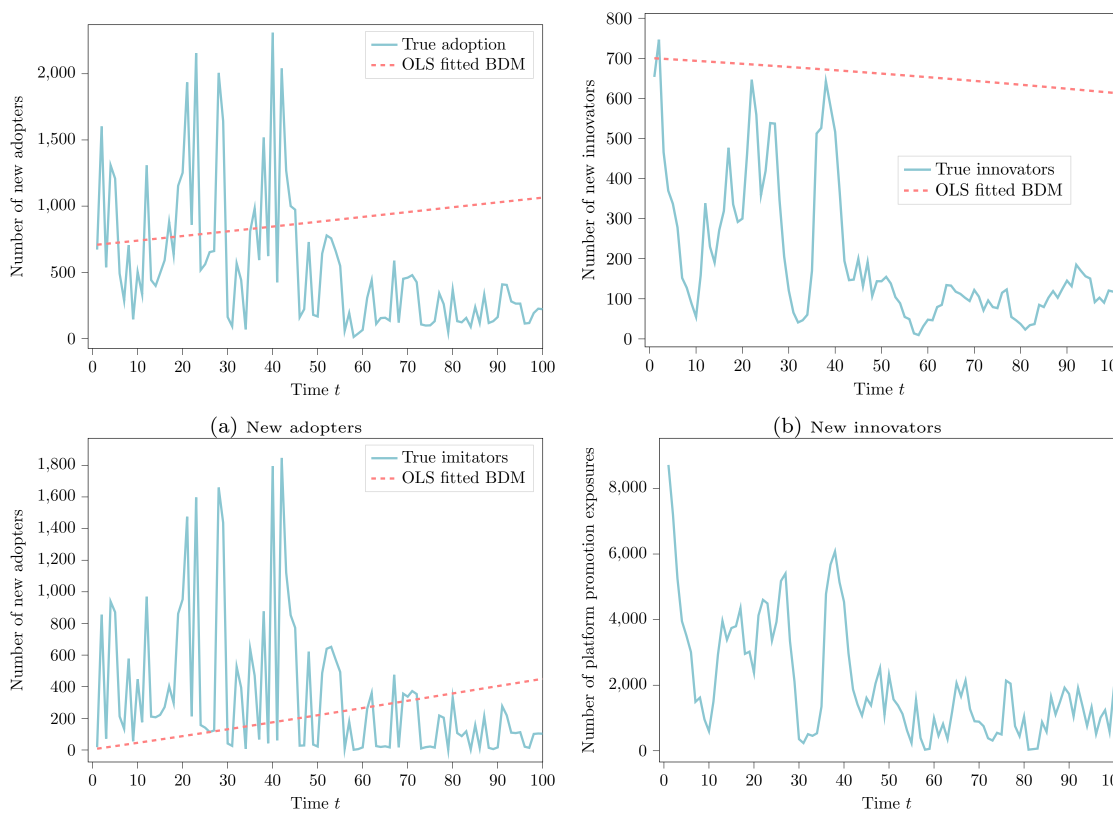

(a) New adopters (b) New innovators

(c) New imitators (d) Platform promotion intensity

Figure 1 Diffusion curves for a piece of online content and the corresponding fitted BDM curves (y axis is scaled by a constant factor)

On the innovator side, the BDM assumes a constant innovative coefficient p and therefore a steady linear decrease of new innovators at each time period. Rather, we observe large variations in real data and quite a sharp turning point on the curve. To further understand the underlying reason, we show the number of times that the video is promoted by the platform in Figure 1d. We observe a similar pattern between this number and the number of new innovators, including a significant drop after $t = 45$. This suggests that the platform's decreased promotion intensity is the primary reason behind the gap between the model's prediction and the actual innovator growth pattern. On the imitator side, it is clear that the BDM predicts an increasing trend, while the real curve exhibits the opposite trend. The number of new imitators also drops after $t = 45$, which coincides well with the time point of the platform's promotion strategy change. In fact, users' interest in sharing decreases quickly after their own adoption. In summary, all of these observations suggest that the BDM may not be well suited for modeling the diffusion process of online content. This motivates us to develop a diffusion model tailored for online content, which will be introduced next. Before closing this discussion, we remark that although we are only showing one example here, the large discrepancy between the fitted BDM and the actual adoption data is widely observed in the data.

3.2. The Online Bass Diffusion Model

The key message conveyed in the previous analysis is that the platform's promotion decisions must be taken into account to capture the diffusion patterns of online content. In this part of the section, we introduce the online Bass Diffusion Model (OBM). We first define the OBM model and focus on a single piece of content. We inherit the notion of innovative and imitative effects from the BDM model while incorporating the platform's promotion decisions. In particular, we assume that the adoption of online content is driven by two forces: (i) The innovative effect: the platform can directly promote the content to users, and users can choose whether to adopt according to their intrinsic value; (ii) The imitative effect: also known as the word-of-mouth effect. After some users adopt the content, they may share it with their friends or inspire other users to search for the content.

We use p and q to denote the intensity of the innovative and imitative effects. We characterize the platform's promotion strategy with promotion probability of x_t, i.e., the platform exposes the content to each user with probability x_t independently. Specifically, nonadopters that are not targeted by platform promotions at time t will only be affected by the imitative effect and adopt the content with probability $q/m \cdot A_{t-1}$ independently. For nonadopters who receive the promotion, their actions will be affected by both the innovative effect and imitative effect. Hence, the adoption probability increases to $(p + q/m \cdot A_{t-1})$. Innovators (resp. imitators) in this procedure are consequently defined as the users who adopt the content with (resp. without) promotion.

Conditional on the number of adopters at time $t-1$, we can write the expected new adopters at time t as

$$\begin{aligned}\mathbb{E}[a_t] &= \left(p + \frac{q}{m}A_{t-1}\right)x_t(m - A_{t-1}) + \frac{q}{m}A_{t-1}(1-x_t)(m - A_{t-1}) \\ &= p(m - A_{t-1})x_t + \frac{q}{m}A_{t-1}(m - A_{t-1}).\end{aligned}$$

Our OBM adopts the deterministic version of the previous equation via fluid approximation. For example, instead of considering that each nonadopter adopts the content with probability $q/m \cdot A_{t-1}$ at time t without being targeted, the fluid approximation assumes that a fraction $q/m \cdot A_{t-1}$ of nonadopters adopt the content deterministically. Thus, abusing the notations, we assume that the number of new adopters at t in the OBM satisfies

$$a_t = p(m - A_{t-1})x_t + \frac{q}{m}A_{t-1}(m - A_{t-1}). \tag{1}$$

As pointed out by Niu (2002), when the market size m is large, the standard deviation of the number of adopters at each time step becomes relatively small. Thus, it is expected that the deterministic process (1) can characterize the expectation of a stochastic process quite well. We conduct simulation experiments to demonstrate the accuracy of the deterministic version in Figure 2. The stochastic simulation curves converge to the deterministic OBM as the market size m increases. When the market size $m = 10\,000$, the curves of the stochastic simulation and deterministic OBM are virtually the same. In practice, the number of users on an online platform far exceeds 10 000.

In practice, there might be some misalignment between the imitative effect and the number of accumulative adopters, as shown in Figure 1c. As we discussed, this is because the incentive for adopters to share content may decay over time. In this case, we introduce the idea of discounted adopters, the details of which are shown in Appendix A.1.

In addition to the incorporation of platform promotion decisions, another essential difference of the OBM from the BDM is its ability to explicitly distinguish between innovators and imitators. With the help of digital technology, the platforms can keep track of the source of each adoption, whether the adopter receives the promotion or not. This provides invaluable information that was never attainable for traditional diffusion models. In Section 5, we develop a new estimation method for OBM that utilizes such information, which outperforms the standard OLS method both empirically and theoretically. Section 6.2 shows that the OBM is a suitable fit for the real adoption curves from the large-scale real-world dataset. Furthermore, we observe that the estimated diffusion parameters p and q are not positively correlated. Namely, the content that is easily adopted when being promoted can fail to diffuse through the social networks, and vice versa. This suggests that it is not trivial to design a promotion strategy that finds a balance between innovative and imitative

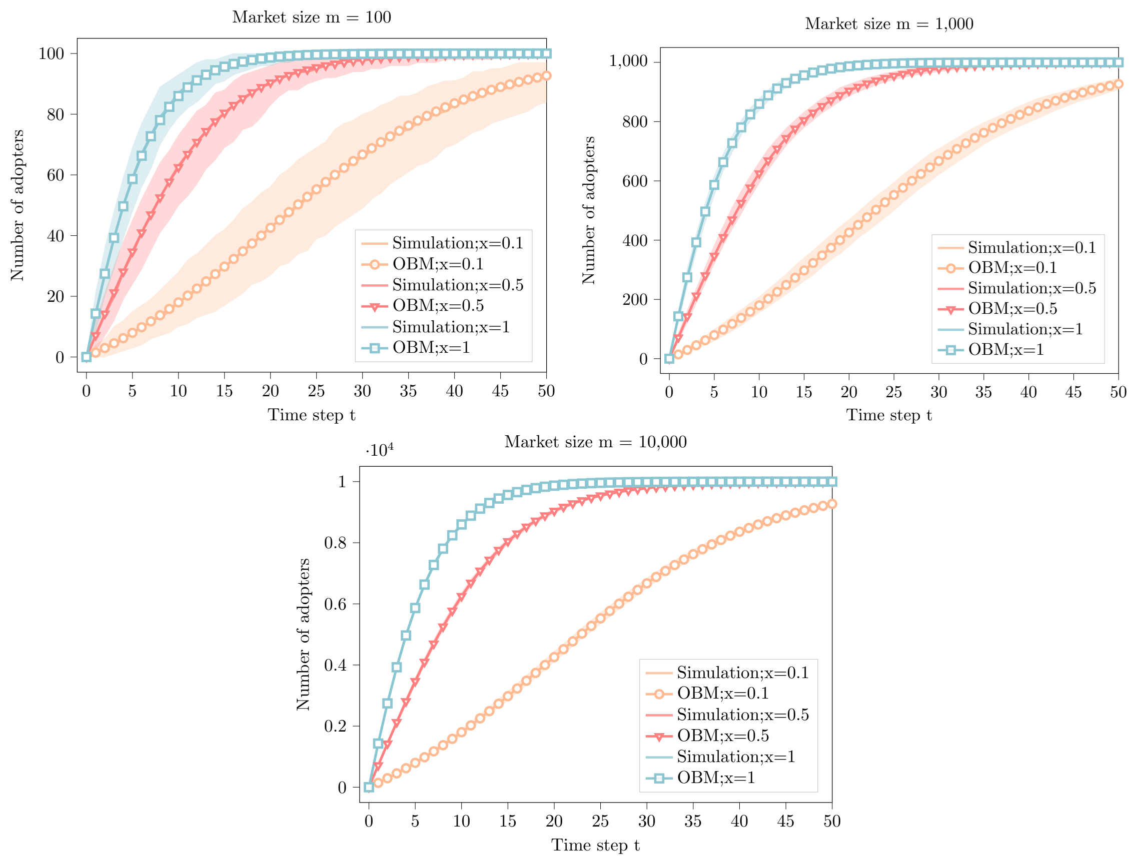

Figure 2 **OBM deterministic approximation versus simulation (The colored shades represents the 95% confidence interval). We set** $p = 0.143$ **and** $q = 0.072$ **and simulate the adoption trajectory for 200 runs.**

effects. We show how to derive a good promotion strategy in Section 4. To avoid distracting the readers, we delay the discussion on the estimation methods of OBM and their results until Section 5.

4. Optimizing Content Adoption

In the previous section, we describe the diffusion model for a single piece of online content. If there is only one piece of content, the platform can promote it to as many users as possible to maximize its adoption. However, in reality, an enormous amount of content in the corpus competes for exposure opportunities; how to decide the promotion probability of each content item becomes a nontrivial problem. In this section, we formulate an optimization problem to determine and promote candidate content in order to achieve the maximum number of total adoptions from all the content.

4.1. Formulation of the Content Generation and Promotion Problem

In this section, we consider the optimization problem for content generation and promotion optimization. By taking the network diffusion effect into account, our aim is to select a candidate subset of content from a large corpus to promote and determine their promotion intensity simultaneously so that the platform can maximize the total number of adoptions after a given fixed period. Only the content that is included in the candidate set can be promoted to users.

We design the content generation and promotion optimization strategy for a fixed time window of length L such that the total number of adoptions is maximized at the end of the L-period time window. The platform possesses a content corpus $\mathcal{V}$. Let $A_{v,t}$ denote the number of adopters for content $v \in \mathcal{V}$ at the beginning of time $t = 1, \ldots, L$. The initial number of adoptions $A_{v,0}$ is known for all content $v \in \mathcal{V}$. $A_{v,t}$ takes values between 0 and m. Without loss of generality, we can assume that $A_{v,0} < m$ for all $v \in \mathcal{V}$. When $A_{v,0} = m$, all users have already adopted content v. Therefore, we can exclude this content from the content corpus $\mathcal{V}$.

The platform makes a two-stage decision. First, it selects a subset $V \subseteq \mathcal{V}$ as the candidate set. Due to practical operational constraints, the candidate set can contain at most K pieces of content. In the second step, the platform decides the promotion probability x_v for each content v in the candidate set V. Specifically, at each time step, the platform promotes content $v \in V$ to each user independently with probability x_v. We assume the adoption process follows the OBM in (1) under the promotion scheme. Hereafter, we use the bold notation to denote the collection of a particular variable for all content in the vector form. For example, $\boldsymbol{x} = (x_v)_{v \in \mathcal{V}}$.

The candidate generation and promotion (CGP) problem can be written as follows:

$$
\begin{aligned}
\underset{\boldsymbol{x}, V}{\text{maximize}} \quad & \sum_{v \in \mathcal{V}} A_{v,L} && && \text{(2a)}\\
\text{subject to} \quad & |V| \leq K, && && \text{(2b)}\\
& A_{v,t+1} = A_{v,t} + p_v(m - A_{v,t})x_v + \frac{q_v}{m} A_{v,t}(m - A_{v,t}) && \forall v \in \mathcal{V} \ \ \forall t = 0, 1, \ldots, L-1, && \text{(2c)}\\
& \sum_{v \in \mathcal{V}} x_v = 1, && && \text{(2d)}\\
& 0 \leq x_v \leq \mathbb{1}\{v \in V\}, && \forall v \in \mathcal{V}. && \text{(2e)}
\end{aligned}
$$

Objective (2a) is the total number of adoptions of all content at the end of the L-step time window. (2b) is the capacity constraint ensuring that at most K pieces of content can be selected. (2c) is the constraint describing the diffusion process according to OBM at different time steps. (2d) is the probability constraint, which requires that the sum of the promotion probabilities equals 1. (2e) ensures that the content has a nonnegative promoting probability. Furthermore, the promotion probability of a piece of content can only be positive if it is included in the candidate set. We perform a static one-time promotion decision throughout the time window, that is, the promotion probability $\boldsymbol{x}$ is kept the same during every L period. Due to practical reasons and operational constraints, the promotion policy cannot be changed frequently. Moreover, the content corpus will be enriched and refreshed continuously over time as users create new content. Therefore, it is more efficient and realistic to consider the static optimization within an appropriate fixed time window L and dynamically optimize this by resolving the problem (with new uploaded content taken into account) periodically.

The CGP problem is difficult to solve in two aspects. On the one hand, the problem is combinatorial in nature. On the other hand, (2c) is a set of nonlinear constraints. When L becomes larger, the difficulty of solving the problem increases accordingly. We state that the CGP problem is NP-hard in Theorem 1. There are no trivial optimization algorithms other than enumerations to solve it unless P=NP. This becomes a critical issue, especially when the content corpus $\mathcal{V}$ is large. This fact motivates us to search for an efficient approximation algorithm that can handle large amounts of content.

Theorem 1 **(NP-hardness)**. *The CGP problem* (2) *is NP-hard.*

Our proof of NP-hardness constructs a reduction from the SUBSET-SUM problem, which is known to be NP-hard. The complete proof is presented in Appendix B.1. In the proof, we use $L=2$ as an example and conclude that for a general L, the CGP problem is NP-hard. Note that when $L=1$, the problem is not NP-hard. In this case, a polynomial algorithm can be obtained by finding the content with the largest $p_v(m-A_{v,0})$ and promoting it with probability 1.

To better analyze the diffusion dynamics, we define $R_v:[0,1]\to\mathbb{R}$ as a mapping from the promotion probability of content v to its total adoptions after L time periods. That is, for content $v\in\mathcal{V}$, $R_v(x_v)=A_{v,L}$, where $A_{v,L}$ follows the step-by-step diffusion constraint (2c). We further define $R:[0,1]^{|\mathcal{V}|}\to\mathbb{R}$ to denote the mapping between the promotion probability of all content and the total adoptions. That is, $R(\boldsymbol{x})=\sum_{v\in\mathcal{V}}R_v(x_v)$. $R(\boldsymbol{x})$ can be regarded as the implicit objective function of the CGP problem. We claim that $R(\boldsymbol{x})$ is strictly monotone and concave in Theorem 2.

Theorem 2 **(Strict monotonicity and concacity)**. *For all* $A_{v,0}=0,1,\cdots,m-1$ *and* $L\geq 1$, *the objective function* $R(\boldsymbol{x})$ *is strictly increasing and strictly concave.*

Theorem 2 shows that given the fixed candidate set, we can determine the promotion probability using convex optimization. This encourages us to design a two-stage algorithm by first evaluating the rewards of a given content set and then selecting the subset with the highest reward.

4.2. A Two-stage Approximation Algorithm for CGP Problem

In this section, we propose an approximation algorithm for the CGP problem. The CGP problem can be decomposed into two stages as a subset selection problem and a promotion probability optimization problem given a fixed candidate set as follows:

$$\max_{V\subseteq\mathcal{V}:|V|\leq K} \quad U(V), \tag{3}$$

where $U(V)$ is the optimal value of the following subproblem:

$$\begin{aligned} \underset{\boldsymbol{x}}{\text{maximize}} \quad & R(\boldsymbol{x}) && \text{(4a)} \\ \text{subject to} \quad & \sum_{v \in V} x_v = 1, && \text{(4b)} \\ & 0 \le x_v \le 1, \quad \forall v \in V. && \text{(4c)} \end{aligned}$$

We show in our analysis that the subset selection problem (3) is a monotone submodular maximization problem with a cardinality constraint. Therefore, the classic greedy algorithm can be utilized to obtain a $(1-1/e)$-approximate solution if there exists an oracle to solve the second stage problem (4) given any $V \subseteq \mathcal{V}$. The greedy algorithm runs in $|\mathcal{V}|K$ calls of the oracle.

It is easy to observe that our second-stage problem (4) is a continuous nonlinear knapsack problem (NKP). Although the general NKP is well studied in the literature, we derive a subroutine tailored for our second-stage problem, building upon the special structure of the problem. This subroutine serves not only as an oracle for the greedy algorithm but also as the most important component to derive the submodularity of the first-stage problem. The proof of the submodularity is nontrivial since the objective function U does not have a closed-form formulation. Moreover, this subroutine can be integrated with the standard greedy algorithm to significantly accelerate the computational time by an order of K. Finally, we can achieve an $(1-1/e)$-approximation solution of the CGP problem with $|\mathcal{V}|K$ calls of the subroutines, where each call of the subroutine runs in $\mathcal{O}(K)$ on average. The overall runtime of our algorithm is $\mathcal{O}\left(|\mathcal{V}|K^2\right)$.

In the following, we first discuss the subroutine for the second-stage problem. We then utilize the subroutine to prove the submodularity of the first-stage problem. Finally, we discuss how we integrate the subroutine with the standard greedy algorithm to accelerate the entire procedure.

4.2.1. Promotion Optimization Given the Content Set Given any candidate set V, we propose a subroutine to capture the structure of the optimal solution. We then develop an $\mathcal{O}(|V|^2)$ algorithm that efficiently finds the promotion decision by exploiting the subroutine.

First, we construct a collection of the second-stage optimization problems (4) parameterized by the candidate set V, which we refer to as the parametrized problem in the following. We refer to the optimization instance with the candidate set V as $\mathcal{I}(V)$ and let $\boldsymbol{x}^*(V)$ and $U(V)$ be the corresponding optimal solution and optimal value, respectively.

The parameterized problem (4) is a continuous nonlinear knapsack problem (NKP). While NKP is a well-studied problem, various studies (Hochbaum 1995, Bretthauer and Shetty 2002) have analyzed its complexity and proposed algorithms to solve it. Instead, our problem is a special case of NKP, that is, a singly constrained convex knapsack problem. There are a wide variety of real-world applications that fall into this special case, such as stratified sampling, manufacturing capacity planning and linearly constrained redundancy optimization problems in reliability networks. Several studies (Nielsen and Zenios 1992, Bretthauer and Shetty 1995, Li and Sun 2006) used the multiplier search method to find the optimal solution based on Karush–Kuhn–Tucker (KKT) conditions. In our parameterized problem, more attributes can be utilized to develop the algorithm; for example, the knapsack constraint is a simplex constraint, and the objective is monotone. We take full advantage of the problem's structure and propose the optimal algorithm with the help of the Lagrangian dual idea. Note that we do not explicitly represent it in the manner of a Lagrangian multiplier. Instead, we use the dual idea to construct the structural property of the parameterized problem and further facilitate the algorithm design for the original CGP problem.

In the following, we present our subroutine for the parameterized problem. The most important ingredient of this subroutine is that for an arbitrary instance $\mathcal{I}(V)$, the partial derivative of the objective function R is the same for each content v at its optimal solution $x^*(V)$. Therefore, the problem is changed to search for a valid value for this partial derivative. We show that the search space can be reasonably divided into $(|\mathcal{V}|+1)$ subintervals. The value is proven to be unique, and thus, it can be efficiently found by enumerating all subintervals.

We define $g_v : [0,1] \to \mathbb{R}$ as the partial derivative of objective function R for content v and g_v^{-1} to be its inverse function. g_v^{-1} is well defined, as there exists a one-to-one correspondence between the promotion probability and the partial derivative of R. g_v and g_v^{-1} may not have closed-form expressions. However, we can calculate their values iteratively. g_v can be generated by iteratively calculating the intermediate reward $A_{v,t}$ and the derivative $dA_{v,t-1}/dx_v$ when $t = 1, 2, \dots, L$ according to (11a). The inverse function g_v^{-1} can be characterized by the bisection method with the realization of g_v. Hereafter, we consider g_v and g_v^{-1} as two given oracles in our subroutine.

For an arbitrary instance $\mathcal{I}(V)$, we define the marginal reward of content $v \in \mathcal{V}$ as the partial derivative of objective function $R(\boldsymbol{x})$ at the optimal solution $x_v^*(V)$. Mathematically, let $\eta_v(V)$ denote the marginal reward of content $v \in \mathcal{V}$, such that $\eta_v(V) = g_v(x_v^*(V))$. A direct observation is that if the optimal solution $x_v^*(V)$ increases, the marginal reward $\eta_v(V)$ will decrease. Furthermore, we define the generalized marginal reward of $\mathcal{I}(V)$ as

$$\tilde{\eta}(V) = \sup_{v \in V} \eta_v(V). \tag{5}$$

In Lemma 1, we show that if a content $v \in V$ is promoted with a positive probability at the optimal solution $x_v^*(V)$, its marginal reward is indeed equal to the generalized marginal reward. As a result, the generalized marginal reward can be used to characterize the optimal solution. All the detailed proofs for this section are shown in Appendix B.1.

Lemma 1 **(Generalized marginal reward)**. *For any instance $\mathcal{I}(V)$, the marginal rewards of all content $v \in V$ such that $x_v^*(V) > 0$ are the same, that is, $\eta_v(V) = \tilde{\eta}(V)$.*

Based on Lemma 1, we show the uniqueness of optimal solution $\boldsymbol{x}^*(V)$ and generalized marginal reward $\tilde{\eta}(V)$ in Theorem 3.

THEOREM 3 **(Uniqueness of optimal solution and generalized marginal reward)**. *For any instance $\mathcal{I}(V)$,*

(i) There exists a unique optimal solution $\boldsymbol{x}^*(V)$.

(ii) Equality (6) holds if and only if $\eta = \tilde{\eta}(V)$, which is the generalized marginal reward.

$$\sum_{v \in \underline{V}_\eta} 0 + \sum_{v \in \tilde{V}_\eta} g_v^{-1}(\eta) + \sum_{v \in \overline{V}_\eta} 1 = 1, \tag{6}$$

where $\underline{V}_\eta = \{v \in V | g_v(0) \leq \eta\}$, $\tilde{V}_\eta = \{v \in V | g_v(1) \leq \eta \leq g_v(0)\}$, *and* $\overline{V}_\eta = \{v \in V | g_v(1) \geq \eta\}$.

With the results of Theorem 3, on the one hand, the optimal solution $\boldsymbol{x}^*(V)$ can be determined by (7) directly once the value of $\tilde{\eta}(V)$ is known, i.e.,

$$x_v^*(V) = \begin{cases} g_v^{-1}(\tilde{\eta}(V)) & \text{when } v \in \tilde{V}_{\tilde{\eta}(V)} \\ 0 & \text{when } v \in \underline{V}_{\tilde{\eta}(V)} \end{cases}. \tag{7}$$

On the other hand, we are able to check whether an arbitrary η equals the generalized marginal reward $\tilde{\eta}(V)$. As long as we can find the η that satisfies (6), we can determine the optimal solution inversely. Based on these properties, we propose Algorithm 1 to obtain the optimal solution of $\mathcal{I}(V)$ by searching for the generalized marginal reward.

For a specific piece of content v, we define the lower bound and upper bound of $\eta_v(V)$ to be $\underline{\eta}_v(V) = g_v(1)$ and $\overline{\eta}_v(V) = g_v(0)$, respectively. The generalized marginal reward $\tilde{\eta}(V)$ can only take values in $[\underline{\eta}(V), \overline{\eta}(V)]$, where $\underline{\eta}(V) = \max_{v \in V} \underline{\eta}_v(V)$ and $\overline{\eta}(V) = \max_{v \in V} \overline{\eta}_v(V)$. When $\eta < \max_{v \in V} \underline{\eta}_v(V)$, we cannot construct a feasible solution that agrees with Lemma 1.

We divide the interval $[\underline{\eta}(V), \overline{\eta}(V)]$ into a number of subintervals such that the sets $\underline{V}_\eta$ and $\overline{V}_\eta$ do not change as long as η stays within that subinterval. Thus, we only need to enumerate the subintervals and find the one that contains $\eta = \tilde{\eta}(V)$ according to Theorem 3. At most $(|V|+1)$, subintervals will be constructed using the thresholds in $\{\overline{\eta}_v(V) : \overline{\eta}_v(V) \geq \underline{\eta}(V), v \in V\}$.

For a given subinterval $[\underline{\eta}, \overline{\eta}]$, let the corresponding two sets be $\underline{V}$ and $\overline{V}$. When $\sum_{v \in \overline{V}} g_v^{-1}(\underline{\eta}) < 1$ (resp. $\sum_{v \in \overline{V}} g_v^{-1}(\underline{\eta}) > 1$), the generalized marginal reward $\tilde{\eta}$ does not lie in this subinterval and $\tilde{\eta} < \underline{\eta}$ (resp. $\tilde{\eta} > \overline{\eta}$). If the generalized marginal reward $\tilde{\eta}$ is included in the subinterval, we deploy a bisection method to find it. Taking the midpoint of the subinterval as η, if $\sum_{v \in \overline{V}} g_v^{-1}(\eta) < 1$, we reduce the subinterval to the left half $[\underline{\eta}, \eta]$; otherwise, we turn to the right half $[\underline{\eta}, \eta]$. Iteratively shrinking the subinterval, we stop when $\sum_{v \in V = \eta} g^{-1}(\eta)$ is close to 1 within the precision.

Algorithm 1: Finding the optimal solution for $\mathcal{I}(V)$

Input: Parameter set V.
Result: Optimal solution $\boldsymbol{x}^*$ and optimal value U.
Sort $\{\overline{\eta}_v(V) : \overline{\eta}_v(V) \geq \underline{\eta}(V), v \in V\} \cup \{\underline{\eta}(V)\}$ in non-decreasing order as $\left[\eta_{[1]}, \eta_{[2]}, \ldots, \eta_{[n]}\right]$.
Initialize $\underline{V} := \emptyset$ and $\overline{V} := V$.
for $i = 1 \rightarrow n$ **do**
    Without loss of generality, assume $\eta_{[i]} = \overline{\eta}_w$.
    w drops out of $\overline{V}$ and enters $\underline{V}$. $\overline{V} := \overline{V} - \{w\}$, $\underline{V} := \underline{V} + \{w\}$.
    Use bisection method to find the solution η to (6).
    if there exists an $\eta \in [\eta_{[i]}, \eta_{[i+1]}]$ that satisfies (6) **then**
        $\tilde{\eta}(V) := \eta$.
        Derive $\boldsymbol{x}^*$ as (7), $U := R(\boldsymbol{x}^*)$. **break**.
    end
end
return $\boldsymbol{x}^*, U$.

The optimality of the solution found by Algorithm 1 directly follows from Theorem 3. Among all the subintervals, only one of them includes the generalized marginal reward $\tilde{\eta}$. Hence, $\tilde{\eta}$ can be found by conducting the bisection method for at most $|V|$ times within that subinterval. The time complexity of the bisection method for content v depends on the range of function g_v and the precision of the solution, which have nothing to do with the scale of the subproblem $|V|$. As a result, the runtime of finding the generalized marginal reward $\tilde{\eta}$ in this subinterval is $\mathcal{O}(|V|)$. Note that the bisection method is used to find the root to (6) in a general form. The algorithm can be more efficient if $g_v^{-1}(\eta)$ has a closed form representation instead. For instance, when $L = 2$, the generalized marginal reward $\tilde{\eta}$ within a subinterval can be derived in $\mathcal{O}(1)$. For subintervals that the generalized marginal reward $\tilde{\eta}$ does not lie in, we only need to check the value of inverse function g_v^{-1} for all $v \in V$ at the lower and upper bounds with time complexity $\mathcal{O}(|V|)$. Therefore, the time complexity of Algorithm 1 can be bounded by $\mathcal{O}(|V|^2)$.

4.2.2. Submodularity of Objective Function We next show the submodularity of the first-stage problem. The submodularity in this problem is not trivial since we need to analyze the relationship between different parameterized instances. We establish Lemma 2 to show that the optimal solutions to parameterized problems have a nested structure over the candidate sets.

LEMMA 2 **(Nested structure)**. *For $V_1 \subseteq V_2 \subseteq \mathcal{V}$, $x_v^*(V_1) \geq x_v^*(V_2)$ and $\tilde{\eta}(V_1) \leq \tilde{\eta}(V_2)$ holds for all $v \in V_1$.*

This nested property is the most important ingredient of submodularity, as the core of submodularity is to show the diminishing marginal gain when adding a new piece of content into the selected subset. Based on the characterization of two instances with nested candidate sets, we then show that $U(V)$ is submodular with regard to set V in Theorem 4.

THEOREM 4 **(Submodularity)**. *$U(V)$ is monotone submodular with respect to V.*

The detailed proof is shown in Appendix B.1. It is trivial to show the monotonicity. The idea of the proof of submodularity is to consider a pair of nested sets V_1, V_2 such that $V_1 \subseteq V_2$ and another piece of content $w \backslash V_2$. We show that in this case, the difference between $(U(V_2 + \{w\}) - U(V_2))$ and $(U(V_1 + \{w\}) - U(V_1))$ can be characterized by the difference between the generalized marginal reward $\tilde{\eta}(V_2)$ and $\tilde{\eta}(V_1)$. Submodularity is then proven by the nested property in Lemma 2.

We now conclude that the CGP problem (2) can be seen as a monotone submodular maximization problem with a cardinality constraint. The well-known greedy algorithm (Nemhauser et al. 1978) provides an $(1 - 1/e)$-approximation. The idea of the greedy algorithm is to iterate K times and choose a piece of content having the largest marginal gain at each iteration. Therefore, we can run Algorithm 1 with $\mathcal{O}(|\mathcal{V}|K)$ times. Because the selected set has a cardinality not larger than K at each iteration, the total time complexity of the approximation algorithm becomes $\mathcal{O}(|\mathcal{V}|K^3)$.

4.2.3. Acceleration with the greedy idea Benefiting from the ordered structure of Algorithm 1, the runtime complexity of the entire CGP problem can be further reduced when integrating the subroutine with the greedy idea. Because the greedy algorithm adds one more piece of content into the selected candidate set at each time, we can utilize the information from previous iterations to speed up the calculation. In particular, let the selected set at iteration k be V_k. We show the Adaptive Greedy Algorithm for an instance $\mathcal{I}(V_k + \{w\})$ where $w \in \mathcal{V} \backslash V_k$ at iteration $k+1$.

Adaptive Greedy Algorithm at Iteration $k+1$

(i) Instead of sorting in Line 1 of Algorithm 1, perform a binary search to insert $\overline{\eta}_w = g_w^{-1}(0)$ into the ordered sequence.

(ii) Instead of enumerating over all k subintervals in Line 3 of Algorithm 1, we only consider the subintervals that have a value not less than $\tilde{\eta}(V_k)$.

As the majority of the ordered sequence remains the same, the binary search in (i) reduces the runtime complexity of sorting from $\mathcal{O}(K \log K)$ to $\mathcal{O}(\log K)$. The other change (ii) reduces the search space for $\tilde{\eta}(V_k + \{w\})$ because by Lemma 2, adding a new content into the candidate set will not decrease $\tilde{\eta}$. In other words, only searching in the space that is greater than or equal to $\tilde{\eta}(V_k)$ can also guarantee optimality. Therefore, whenever we add content w, we do not repeatedly check the previous examined subintervals. After all K iterations, at most K subintervals will be tested for each content. Overall, the time complexity of the Iterative Algorithm 1 is reduced to $\mathcal{O}(|\mathcal{V}|K^2)$.

5. Parameter Estimation

In this section, we propose a double OLS (D-OLS) method for estimating the parameters p and q from real adoption data, highlighting the value of the platform's capability to distinguish between innovators and imitators in estimations. We show that the D-OLS estimators are statistically consistent and achieve much smaller asymptotic variances compared with the conventional OLS method.

Parameter estimation has been a problem that been extensively discussed for BDM. Bass (1969) first estimated the problem using the OLS method. However, in the presence of time-series data and with multicollinearity between variables, the estimators usually have large variances and biases. Schmittlein and Mahajan (1982), Srinivasan and Mason (1986), Satoh (2001) applied maximum likelihood estimation (MLE) and nonlinear least square (NLS) to avoid these issues and obtained better estimation results. However, both MLE and NLS require representing the number of accumulated adopters at each time step as an explicit function of time t so that they can rule out the autocorrelation between the data samples. For our proposed OBM, the closed-form expression no longer exists, as the promotion probability is controlled by the platform and may vary over time. Therefore, MLE and NLS are not applicable in our setting. In our discussion, we focus on the OLS method for estimation.

Different from the estimation for BDM, in the estimation of OBM, we only focus on two diffusion parameters p and q and assume that the market size m is known. Conventionally, the data that we can observe include $\{A_{v,t}\}_{t=0}^{T-1}$, $\{x_{v,t}\}_{t=1}^{T}$, and $\{a_{v,t}\}_{t=1}^{T}$ for all $v \in \mathcal{V}$. The OLS method assumes the following relationship between the number of new adopters and the innovative/imitative potential:

$$a_{v,t} = p_v \cdot x_{v,t}(m - A_{v,t-1}) + q_v \cdot \frac{A_{v,t-1}}{m}(m - A_{v,t-1}) + \epsilon_{v,t},$$

where $\epsilon_{v,t}$ is random noise. For notation simplicity, let $z_{v,t,1} = m - A_{v,t-1}$ and $z_{v,t,2} = \frac{A_{v,t-1}}{m}(m - A_{v,t-1})$. The OLS method then regresses the number of new adopters $\boldsymbol{a}$ on $\boldsymbol{z}_1$ and $\boldsymbol{z}_2$.

Similar to the OLS estimation for BDM, the issue of the multicollinearity between attributes and autocorrelation still exists in the OLS method for OBM. As a result, the OLS estimators for OBM can be biased and have large variances. With the help of online content platforms, we are able to improve the estimation results by including additional information about adopters. Specifically, we can distinguish whether an adopter is an innovator or an imitator by identifying whether the user has been targeted for promotion or not. Let the number of new innovators and imitators for content v at time t be $a_{v,t}^{\text{in}}$ and $a_{v,t}^{\text{im}}$. Therefore, the data that we can observe include $\{A_{v,t}\}_{t=0}^{T-1}$, $\{x_{v,t}\}_{t=1}^{T}$, $\{a_{v,t}^{\text{in}}\}_{t=1}^{T}$, and $\{a_{v,t}^{\text{im}}\}_{t=1}^{T}$ for all $v \in \mathcal{V}$. We propose a double-OLS (D-OLS) method to obtain better estimators for OBM based on the following relationships for innovators and imitators:

$$a_{v,t}^{\text{in}} = p \cdot x_{v,t} z_{v,t,1} + q \cdot x_{v,t} z_{v,t,2} + \epsilon_{v,t}^{\text{in}}, \tag{8a}$$

$$a_{v,t}^{\text{im}} = q \cdot (1 - x_{v,t}) z_{v,t,2} + \epsilon_{v,t}^{\text{im}}, \tag{8b}$$

where (8a) focuses on the potential innovators that have been targeted for promotion while (8b) focuses on the potential imitators; $\epsilon_{v,t}^{\text{in}}$ and $\epsilon_{v,t}^{\text{im}}$ are random noises.

Our D-OLS method estimates the innovative and imitative coefficients separately:

(i) Estimate $\hat{q}^{\mathrm{D}}$ from (8b) via OLS, and obtain

$$\hat{q}^{\mathrm{D}} = \frac{\sum_{(v,t)} \left[(1-x_{v,t})z_{v,t,2}a^{\mathrm{im}}_{v,t}\right]}{\sum_{(v,t)} \left[(1-x_{v,t})z_{v,t,2}\right]^2};$$

.

(ii) Replace q in (8a) with the D-OLS estimator $\hat{q}^{\mathrm{D}}$. Estimate $\hat{p}^{\mathrm{D}}$ from (8a) via OLS, and obtain

$$\hat{p}^{\mathrm{D}} = \frac{\sum_{(v,t)} \left[x_{v,t}z_{v,t,1}(a^{\mathrm{in}}_{v,t} - \hat{q}^{\mathrm{D}}x_{v,t}z_{v,t,2})\right]}{\sum_{(v,t)} \left(x_{v,t}z_{v,t,1}\right)^2}.$$

The intuition behind the D-OLS is that it can alleviate the problem of multicollinearity with the additional information acquired. Separating the estimation of two coefficients helps reduce the variance of the estimators and improves the prediction accuracy. While it is impossible to eliminate the autocorrelation, we can alleviate this issue by including the adoption data of an ensemble of the content. That is, for generalization purposes, we often assume that a collection of content (i.e., with similar characteristics or within the same category) shares the same pair of parameters. Including adoption trajectories of different content can reduce the correlation in time. In the extreme case, if we only include one observation per piece of content in the training set, the estimator will become unbiased. We give a more rigorous explanation of this in the next section by analyzing the asymptotic bias and variance of the D-OLS estimation.

5.1. Asymptotic Properties

In this section, we discuss the asymptotic properties of the D-OLS estimators when the number of observations tends to infinity. We show that the D-OLS estimators are consistent; that is, the estimators converge to their true value as the number of observations increases. Additionally, D-OLS estimators have smaller asymptotic variances than OLS estimators, which illustrates the advantage of eliminating multicollinearity.

For theoretical purposes, we assume that the promotion probability $x_{v,t}$ is independently sampled from a distribution. In reality, the promotion probability $x_{v,t}$ can be endogenous, that is, the platform will determine the promotion policy based on the value of p, q and A. To guard against endogeneity, the platform can reserve a small portion of the content and apply a fixed promotion policy for estimations. Hereafter, we use the notation x, z_1 and z_2 without the subscription denoting content and time as the random variable that characterizes the distribution of the corresponding attributes in the entire dataset. We assume the OLS random noise $\epsilon_{v,t}$ is independently and identically sampled from $\mathcal{N}(0,\sigma^2)$. To rigorously align (8) and the OLS formulation to facilitate the following discussion, we assume random noise $\epsilon^{\mathrm{in}}_{v,t}$ follows $\mathcal{N}\left(0,\mathbb{E}[1-(1-x)^2]\sigma^2\right)$ and $\epsilon^{\mathrm{im}}_{v,t}$ follows $\mathcal{N}\left(0,\mathbb{E}[(1-x)^2]\sigma^2\right)$ independently. Hence, $\epsilon_{v,t} = \epsilon^{\mathrm{in}}_{v,t} + \epsilon^{\mathrm{im}}_{v,t}$ follows $\mathcal{N}\left(0,\sigma^2\right)$.

The number of observations can increase in two different ways, one is to observe T samples for a piece of content and let T increase as time goes by; the other one is to observe a fixed T number of samples for each content but increase the number of content N in the same category. The former type of dataset growth results in a large autocorrelation in the data samples, while the latter alleviates the impact of an autocorrelation by increasing the pool of content. Theorem 5 below shows that when either T or N tends to infinity, the D-OLS estimation yields consistent estimates of both coefficients p and q. The proof and its required mild assumptions are given in Appendix B.2.

Theorem 5 **(Asymptotic consistency)**. *The D-OLS method estimates the diffusion coefficients p and q consistently when the number of data samples increases either in time (i) or in ensemble (ii).*

(i) With mild assumptions, we observe T samples of the same content at different times. The number of data samples increases as the observing horizon T increases.

(ii) Observe a fixed T sample for a collection of N content. The number of data samples increases as the number of content N increases.

In addition to statistical consistency, the D-OLS estimators can also achieve smaller asymptotic variances. The intuition is that the D-OLS estimation isolates the variation of two different estimators. Hence, the asymptotic variances of both estimators will decrease, especially when multicollinearity exists in the OLS formulation. To rule out the impact of autocorrelation on asymptotic variance, we consider the growing dataset as the number of content N tends to infinity and show the asymptotic variance for both the D-OLS and OLS estimators in Theorem 6.

Theorem 6 **(Asymptotic variance)**. *As the number of observed content N increases,*

(i) The asymptotic variances of D-OLS estimators $\hat{p}^D$ and $\hat{q}^D$ are $\frac{1}{\mathbb{E}[x^2 z_1^2]}\left(1-\mathbb{E}[(1-x)^2]\right)\sigma^2$ and $\frac{1}{\mathbb{E}[z_2^2]}\sigma^2$ respectively.

(ii) The asymptotic variances of OLS estimators $\hat{p}^{OLS}$ and $\hat{q}^{OLS}$ are $\frac{1}{\mathbb{E}\left[x^2 z_1^2\right]}(1+\kappa)\sigma^2$ and $\frac{1}{\mathbb{E}\left[z_2^2\right]}(1+\kappa)\sigma^2$ respectively, where $\kappa = \frac{\mathbb{E}[z_1 z_2]^2}{\mathbb{E}\left[z_1^2\right]\mathbb{E}\left[z_2^2\right]-\mathbb{E}[z_1 z_2]^2}$ is a positive constant.

The theorem is proven in Appendix B.2.

By the Cauchy-Schwarz inequality, we note that $\kappa \geq 0$ always holds. Thus, the asymptotic variances of the OLS estimators are notably larger than those of the D-OLS estimators, and the ratio of the increment is at least κ. When random variables z_1 and z_2 have a large linear correlation, the gap between the two variances becomes larger as the denominator approaches 0.

In our setting, z_1 and z_2 are not perfectly correlated, so the variance of the OLS estimator will not become arbitrarily large. However, we will show that the ratio of the increment is still not negligible. Here, we consider the basic case when the discount factor $\gamma = 1$, and we have $z_1 = m - A$ and $z_2 = \frac{A(m-A)}{m}$. As time-series adoption data often include adopters at different levels, to illustrate the intuition, we assume that the number of adopters A is uniformly distributed between 0 and m in the observed dataset. It then follows that

$$\mathbb{E}[(m-A)^2 A]^2 = \frac{1}{144} m^4 \qquad \text{and} \qquad \mathbb{E}[(m-A)^2]\mathbb{E}[(m-A)^2 A^2] = \frac{1}{90} m^4,$$

and therefore the ratio of increment becomes at least

$$\frac{\mathbb{E}\left[z_1 z_2\right]^2}{\mathbb{E}\left[z_1^2\right]\mathbb{E}\left[z_2^2\right] - \mathbb{E}\left[z_1 z_2\right]^2} = \frac{\mathbb{E}[(m-A)^2 A]^2}{\mathbb{E}[(m-A)^2]\mathbb{E}[(m-A)^2 A^2] - \mathbb{E}[(m-A)^2 A]^2} = \frac{8}{3}.$$

This result indicates that in the basic case, the asymptotic variances of OLS estimators increase at least 267% compared with the D-OLS estimators. Therefore, the power of observing two types of adopters and estimating separately can largely reduce the variance of the estimators.

In Figure 3, we present computational examples of the asymptotic properties for the D-OLS and OLS estimators. The example considers the content with the same pair of coefficients $(p = 0.143, q = 0.072)$ in a market of $m = 10\,000$. We simulate the adoption process for each content item and randomly pick 10 samples from each content item . With this dataset, we estimate p and q with both methods. Figure 3a shows the estimation error, measured using the Euclidean distance between the estimators and true value $\sqrt{(p-\hat{p})^2 + (q-\hat{q})^2}$. We observe that the estimation error of the D-OLS estimators shrinks quickly and is relatively smaller than that of the OLS estimators. Figures 3b and 3c present the value of the estimators, with the black dotted curves representing the true values of p and q. The estimators converge toward their respective true values, and the 95% confidence interval of OLS estimators is much larger, echoing the result of Theorem 5 and Theorem 6.

6. Numerical Results

In this section, we conduct a counterfactual analysis based on our OBD model with parameters estimated using a real-world dataset from a large-scale video-sharing platform in China. Our numerical experiments include the estimation of diffusion parameters, a comparison between different estimation methods, and a performance evaluation of the adaptive greedy promotion policy.

6.1. Data Overview

Our analysis is built upon a dataset from one of the most famous video-sharing platforms in China. Similar to TikTok, users record and share their lives on the platform using short videos with a length of less than 1 minute. In 2020, the platform had an average of 3 billion daily average users and over 20 billion videos in total. Active users spend an average of more than 100 minutes daily

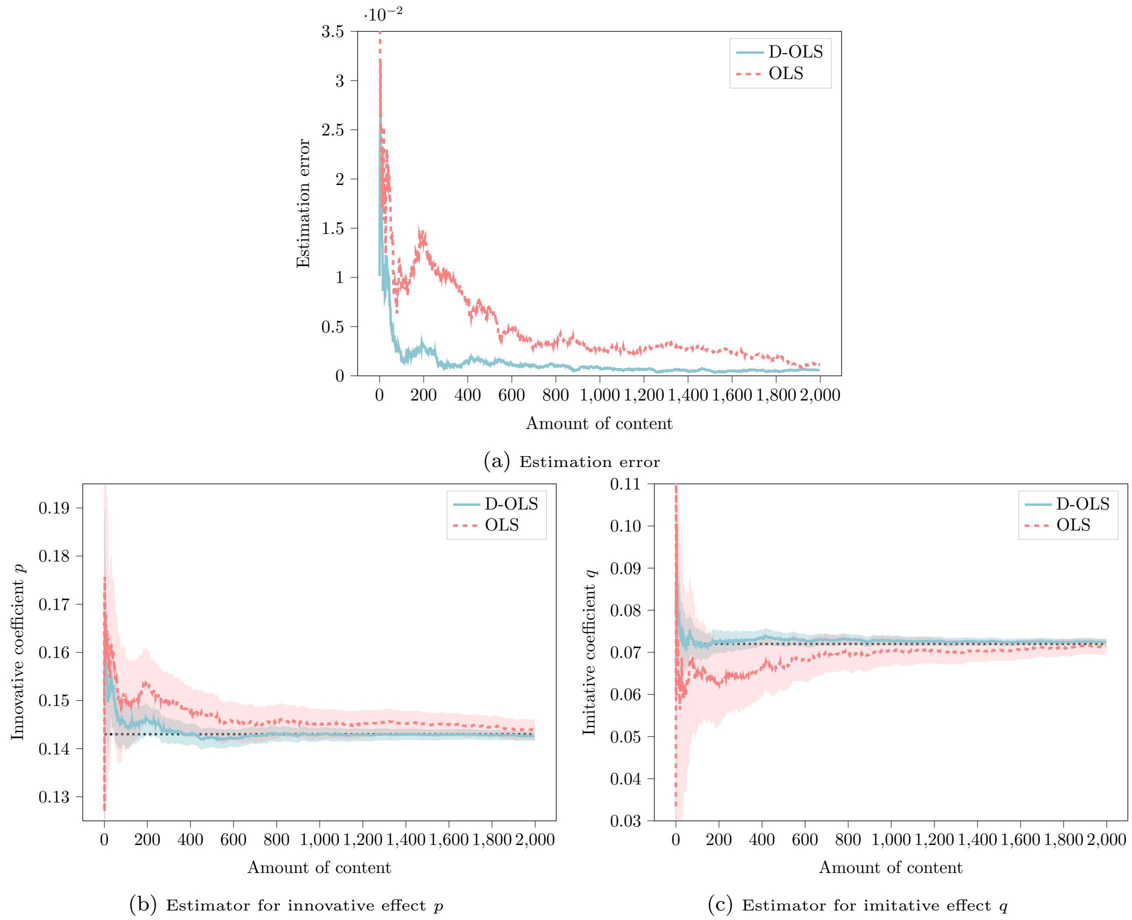

Figure 3 **The asymptotic properties of estimators $\hat{p}$ and $\hat{q}$ as the number of observations increases. (The shaded area denotes 95% confidence interval for estimators.)**

on the platform. The platform operates as follows: The users are displayed with videos promoted by the platform once they log in. They can click to watch videos that they are interested in. When a user watches a specific video, there is a share button for him to share the video with friends.

The dataset we obtained comprises the behavior log data of 46 444 short videos sampled from 518 646 users for 20 days (7/1/2020-7/20/2020). The raw log data include the timestamped records of videos promoted to users and the responses in terms of clicks. We consider the time granularity of the data samples to be hourly, i.e., each time step represents an hour. To be specific, within each hour, we observe a list of users who receive the promotion of a piece of content and another list of users who click on that content. Therefore, we can clearly identify whether an adopter is an innovator or imitator according to whether she receives the promotion or not.

In addition, the dataset contains information on the video category. The videos are categorized by the platform according to their content, such as travel, education, game, etc. To ensure that the adoption records contain the complete diffusion process from the very beginning for the selected content, we selected the videos that were newly uploaded to the platform within the 20 days (7/1/2020-7/20/2020) from 61 categories in our experiment.

6.2. Model Calibration

In this section, we estimate the parameters from the dataset. We show the discount factor in a real diffusion as well as the distribution of the diffusion coefficients p and q for online content. The dataset includes 11 542 338 content-time specific samples in total. We estimate the diffusion parameters (p, q) for each category, the details of which are contained in Appendix C.1.2. The mean absolute percent error (MAPE) between the true value and predicted value of new adopters $\frac{1}{|\{(v,t)\}|}\sum_{(v,t)}\frac{|a_{v,t}-\hat{a}_{v,t}|}{a_{v,t}}$ is used to measure the performance.

In practice, the OBM fits better with the discounted adopters. In our experiments, we assume an exponential-smoothed decay of adopters' sharing incentive, i.e., $\tilde{A}_t = \sum_{\tau=1}^{t-1}\gamma^{t-\tau-1}a_\tau$. We choose the discount factor $\gamma = 0.26$, which has the best average performance among all the categories. More details on the selection of the discount factor are shown in Appendix C.1.3.

Estimation performance: We estimate the diffusion coefficients for OBM using the OLS and D-OLS methods, respectively. Overall, the weighted average MAPE among all categories is 22.76% for the D-OLS estimation and 23.20% for the OLS estimation, where a relative improvement of 1.97% is achieved. Furthermore, we compare the performance of the OBM with that of the classical BDM. We find that the weighted average MAPE for a fitted BDM is 107.05%, which is much larger than OBM with either an OLS or D-OLS estimation. This result implies that BDM is not suitable for online content diffusion, while the OBM with the D-OLS estimation method provides the best fit.

To further illustrate the differences between the OLS and D-OLS methods for OBM, we examine the MAPE of each category. 51 out of 61 categories (83.6%) show that D-OLS outperforms OLS. Figure 4 shows the distribution of the relative MAPE improvement among all the categories. For different categories, especially those that have a relatively smaller number of data samples, we can see a much larger improvement in performance. Table 1 reports the out-of-sample MAPE of two categories as an example.

Table 1 Out of sample MAPE for two selected categories of content

	Observations	D-OLS	OLS	Relative MAPE improvement
Category 1	13 998	0.1630	0.1897	14.06%
Category 2	107 070	0.3225	0.3316	2.75%

We then fit the adoption curves using the estimated coefficients. Figure 5 shows the fitted curves for both the D-OLS and OLS estimations as well as the true diffusion curves. OBM can effectively

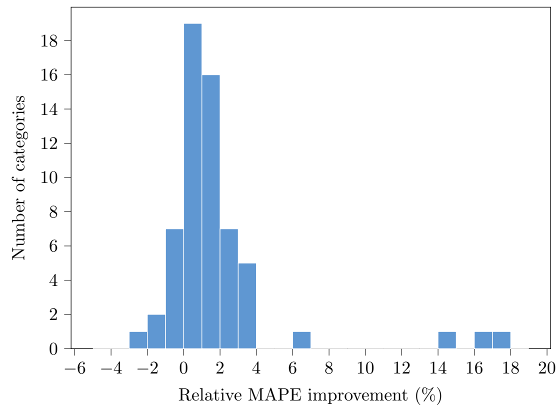

Figure 4 **Distribution of the relative MAPE improvement of D-OLS based on OLS method for OBM**

characterize the diffusion behavior of online content, while D-OLS provides a better quality of prediction.

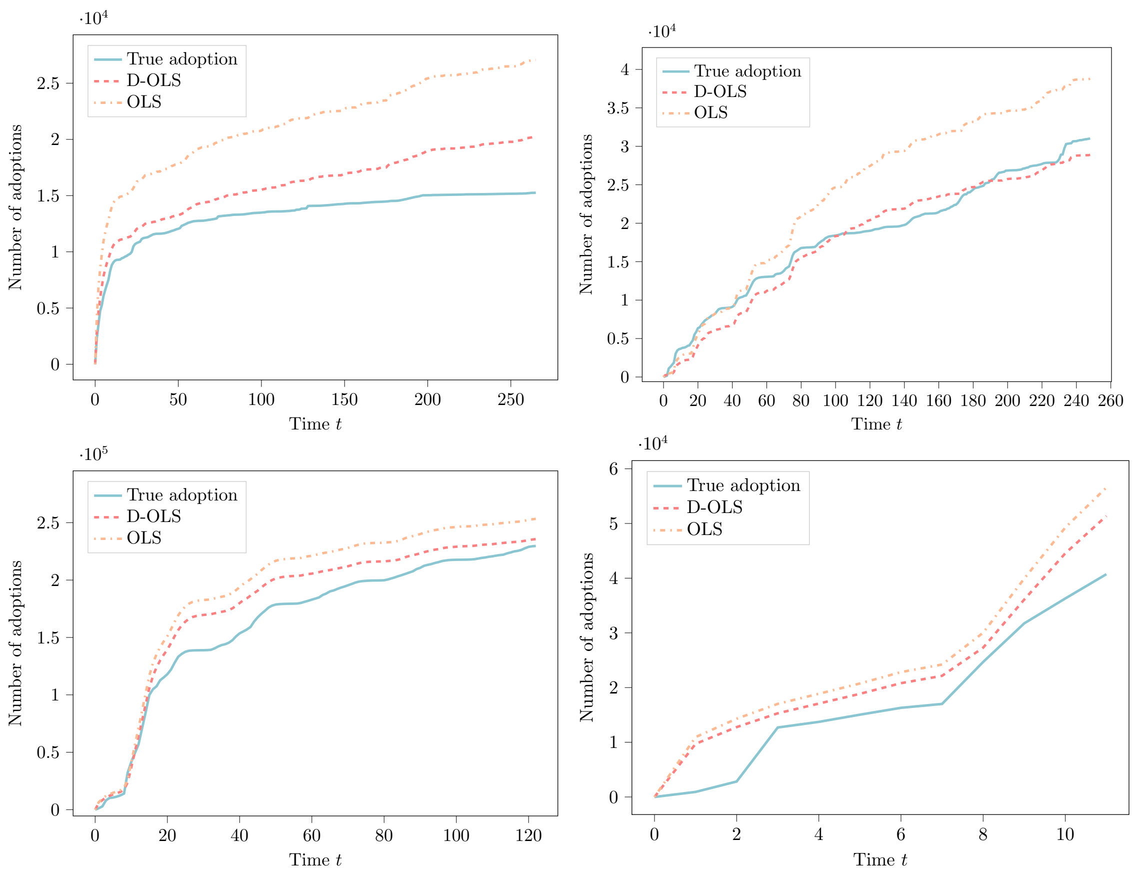

Figure 5 **Diffusion curves for two online content categories and the corresponding fitted D-OLS/OLS curves (Upper figures come from category 1 and lower figures come from category 2, y axes are scaled by some constant factors)**

Distribution of p and q: Figure 6 demonstrates the distribution of $\hat{p}^{\mathrm{D}}$ and $\hat{q}^{\mathrm{D}}$ estimated from

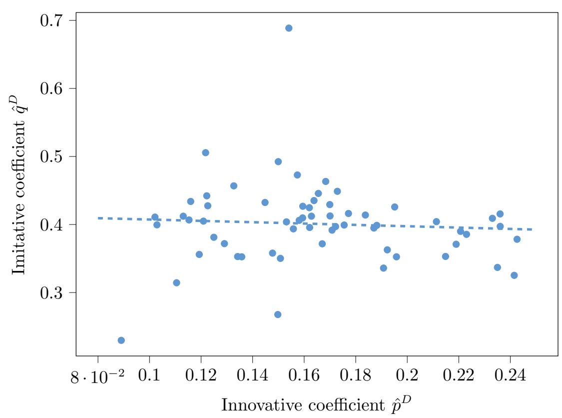

Figure 6 **Distribution of estimated innovative coefficient p and imitative coefficient q. Each point in the scatter plot represents a content category. (The dashed line is fitted to all points via OLS.)**

the D-OLS method across the 61 categories. Heterogeneity is observed among different content categories. From Figure 6, we can also observe a slightly negative correlation ($\rho = -0.064$) between p and q for the same content category. This implies that the content that attracts users directly via promotion may not necessarily lead to a higher diffusion effect. All the observations emphasize the indispensable role of promotion decisions in the OBM.

In traditional BDM for consumption goods, p is usually far less than q, with an average value of $p = 0.03$ and $q = 0.38$ (Sultan et al. 1990). In our OBM, the average values are $p = 0.16$ and $q = 0.40$. We note that the assumption $p + q \leq 1$ is satisfied for all the content categories. The innovative coefficient p has a larger value and wider range, while the imitative coefficient q is relatively smaller when taking discount factor γ into account. However, the result does not necessarily mean that the diffusion power of online content is weaker than that of consumption goods. The low adoption cost of online content encourages users to click the content in a timely manner when targeted by the platform, while the rapid update of online content makes it difficult to become consistently attractive. Thus, innovators account for a much larger proportion of adopters. If we compare the timely diffusion, the imitative effect also has a relatively larger magnitude.

6.3. Experiments on the Adaptive Greedy Algorithm

In this section, we use the parameters estimated from the dataset as our ground truth and simulate user behavior as well as the platform's decisions with different promotion policies. For all experiments in this section, we use the same collection of content categories as the real-world dataset and assume that the content distribution is uniform among all the categories.

6.3.1. Computational Efficiency and Accuracy of Adaptive Greedy Algorithm We first investigate the accuracy and efficiency of our algorithm by comparing how the optimality gap and CPU execution time change with respect to the candidate set size K and the entire content corpus size $|\mathcal{V}|$. We set market share $m = 10\,000$ and time window L from 2 to 5. For the experiments with respect to K, we fix $|\mathcal{V}| = 100$ and let $K \in \{10, 20, 30, 40, 50\}$; For the experiments with respect to $|\mathcal{V}|$, we fix $K = 50$ and let $|\mathcal{V}| \in \{200, 400, 600, 800, 1000\}$. For each test instance, we tested over 30 randomly generated adoption states. Tests are performed over the approximation results of the greedy algorithm and the optimal results of the mixed integer program of the Gurobi solver. When L is greater than 2, the solver is not able to find the optimal solution. We set the time limit to 300 seconds and compare it against the upper bound found by the solver. We evaluate the performance of our method using the percentage of upper bound achieved.

Experiment result: Figure 7 shows the optimality gap for different test instances. On average, the Adaptive Greedy Algorithm has a small optimality gap. It achieves on average more than 96% of the upper bound in all cases. Figure 8 shows the execution time in CPU seconds. We observe that the runtime of the Adaptive Greedy Algorithm grows almost linearly with K and $|\mathcal{V}|$. In contrast, the solver takes much longer to solve the MIP problem. Apart from the exponential growth of time with regard to the problem scale, the high-order nonlinearity of the objective also causes an unpredictable increase in the execution time when L is large. This is also the reason that we cannot achieve the exact optimal value. Thus, our algorithm has tremendous advantages in practice. The numerical results are presented in Appendix C.2.

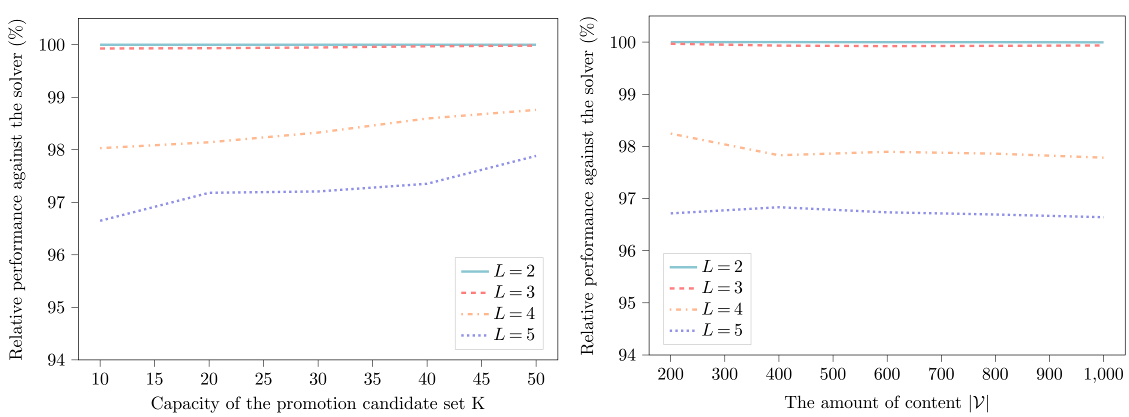

Figure 7 **Accuracy test: left is the result for different K and right is the result for different $|\mathcal{V}|$**

6.3.2. Choice of Promotion Time Period L When applying the static policy with promotion time window L to a longer time horizon, we will update the promotion scheme every L time

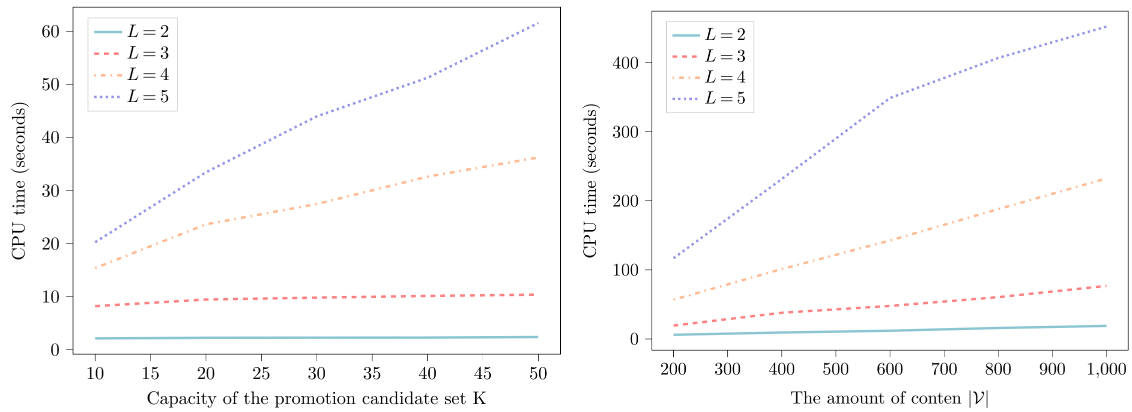

Figure 8 **Efficiency test: left is the result for different K and right is the result for different $|\mathcal{V}|$**

step based on the real-time adoption level. In this section, we compare the long-term reward of promotion policies with different time windows L.

To measure the long-term reward, we will measure the performance at a time horizon T, which is much longer than L. However, based on the assumption of OBM, all the users will adopt the content regardless of the promotion scheme as time goes to infinity. In practice, the platform wants to achieve large adoptions within a limited time so that the content corpus can be updated with the latest content. Therefore, the time step T is chosen to be a moderate value. We start at $t=0$, where the adoption state $A_{v,0}=0$ for all content $v \in \mathcal{V}$. We evaluate the rewards of the promotion policies with different time windows L at the end of the planning horizon $t=100$. We set market share $m=10\,000$, $|\mathcal{V}|=1\,000$ and let $K \in \{50, 100, 200, 300\}$. For each policy, we tested over 30 randomly generated content corpora $\mathcal{V}$.

Experiment results: In Figure 9, we illustrate the diffusion results for different promotion policies. Figure 9a shows the number of adopters at $T=100$. $L=1$ can be considered as a benchmark since it is the policy that neglects the imitative effect and is generally used in practice. Even in the worst case ($K=50$), the reward of the best promotion policy makes at least a 12.84% improvement compared with the base policy $L=1$. Furthermore, we note that the best promotion period L also depends on the capacity K of the platform. When the capacity is small, ($K=50,100$), planning ahead for a small L, such as 2 or 3, can achieve the best performance. When the platform is able to promote more content ($K=200,300$), a longer time period L will help to increase total adoptions. Thus, the best time period can be set to 5 or even larger. The intuition behind this is that a longer promotion time window exploits the imitative effect more thoroughly but suffers from the inflexibility of the promotion scheme. When the capacity is small, the adoption procedure of the content in the candidate set will speed up. Therefore, quick updates of the promotion scheme are preferred.

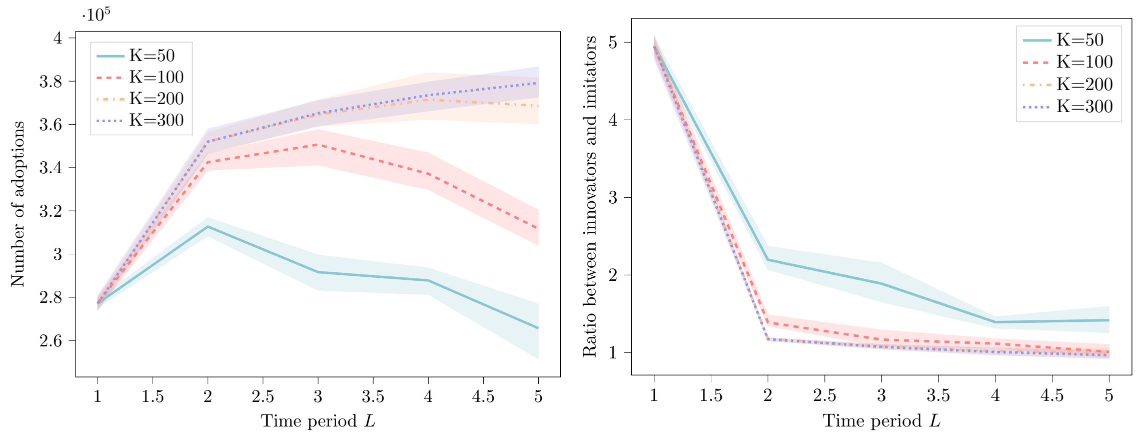

(a) Cumulative reward (b) Ratio between innovators and imitators

Figure 9 The adoption results at $T = 100$ vs promotion time period L. (The shaded area denotes 95% confidence level, y axis of left subfigure is scaled by a constant factor)

Figure 9b shows the composition of the adopters. We use the ratio between innovators and imitators to indicate the differences. When $L = 1$, the number of innovators is notably greater than the number of imitators. When L increases, the ratio becomes stable at approximately 1, where the innovators and imitators have almost the same size. It is interesting to find that this ratio in the real dataset is approximately 3.35. It shows the evidence that diffusion is not sufficiently considered in the current promotion policy, as this value is between the tested policies with $L = 1$ and $L = 2$.

6.3.3. Compare Adaptive Greedy Algorithm Performance with Benchmarks We evaluate the cumulative reward of the Adaptive Greedy Algorithm over periods $\mathcal{T} = \{1, 2, \ldots, 100\}$ with the benchmark policies defined as follows. We set market share $m = 10\,000$ and consider the setting with $K = 200$ and $L = 4$, which is empirically a good promotion scheme as shown in the previous section. For each benchmark, we tested over 30 randomly generated content corpora $\mathcal{V}$.

Benchmark policies: We define several benchmarks that are commonly used in industry practice. For a fair comparison, we simulate the policy using the same adoption process as our algorithm and compare the generated virtual rewards.

CGP with the Adaptive Greedy Algorithm (ADG): This benchmark is the adaptive greedy algorithm discussed in Section 4.2.2.

Candidate Generation by Popularity (POP): This benchmark considers a heuristic candidate generation strategy by selecting K pieces of content that are the most popular in the meantime. In other words, we first choose a set of content that has the most adopters A_v from the corpus and then solve the parameterized CGP problem. This benchmark illustrates the *rich-get-richer* principle in reality.

Candidate Generation by Attractiveness (ATT): This benchmark considers a heuristic candidate generation strategy by selecting K pieces of content that are the most attractive. In other words, we choose a set of content that has the largest innovative potential $p_v(m - A_v)$ and then solve the parameterized CGP problem. This benchmark overemphasizes the innovative effect of the content, which aims to attract more immediate adoptions.

CGP without the diffusion effect (NoD): This benchmark considers promoting the content without considering the network effect. This is equivalent to the CGP formulation when $L = 1$. It is a common practice in the industry that ignores the imitative effects when promoting the content.

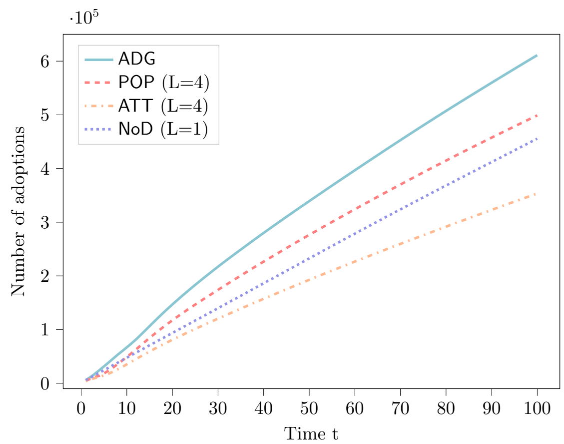

Figure 10 **Algorithm performance: compared with three benchmark policies (y axis is scaled by a constant factor)**

Table 2 **Performance of promotion policies**

Promotion policy	Final number of adoptions	% of gain of our method
ADG	611 102	-
POP (L=4)	498 926	22.48%
ATT (L=4)	353 551	72.85%
NoD (L=1)	455 558	34.14%

Experiment result: Figure 10 shows the cumulative adoptions for different policies. The numerical results are presented in Table 2. Our algorithm outperforms three benchmarks by 22.48%, 72.85%, and 34.14%, demonstrating considerable improvements. Compared with the three benchmarks, we show the advantages of our algorithms in different aspects. The comparison with POP and ATT suggests that the candidate generation procedure cannot trivially consider a single indicator of the content, such as historical popularity and attractiveness. It also illustrates the harmful effect of the *rich-get-richer* principle. The comparison with NoD emphasizes the importance of considering the network diffusion effect when evaluating the total adoptions. These results highlight the significance of considering both the candidate generation procedure and the network diffusion effect for the platform content promotion problem.

7. Conclusion

In this study, we explore the content promotion problem under the diffusion effect for online content platforms. We propose a novel diffusion model to capture the diffusion behavior of online content. Based on the diffusion model, we formulate the candidate generation and promotion (CGP) problem. The CGP problem is NP-hard, so we propose an approximation algorithm that exploits the problem structure. We then propose a double OLS estimation procedure for the diffusion coefficients. Finally, we use a real-world dataset to validate our model and evaluate the performance of the algorithms. In particular, we find empirical evidence that shows that considering the diffusion effect in promotion optimization is of great importance. We also observe a large improvement of the adaptive greedy algorithm by using benchmark comparisons. There are several future directions for this study. First, among the population, users may have different preferences for the same content. One can extend the model to multiple user types. However, the orderly structure of the parameterized variants will no longer exist. The problem becomes a more general NKP problem. Further exploration will be required to efficiently solve the optimization problem. Second, online content platforms have an abundance of user and content information, which offers opportunities to consider the problem in a contextual setting.

References

Agrawal, S., Yin, S., and Zeevi, A. (2021). Dynamic pricing and learning under the bass model. In Proceedings of the 22nd ACM Conference on Economics and Computation, pages 2–3.

AMZScout (2021). Amazon statistics for 2021 and the latest facts. `https://amzscout.net/blog/amazon-statistics/`. Accessed: 2022-03-11.

Anandhan, A., Shuib, L., Ismail, M. A., and Mujtaba, G. (2018). Social media recommender systems: review and open research issues. IEEE Access, 6:15608–15628.

Arora, A., Galhotra, S., and Ranu, S. (2017). Debunking the myths of influence maximization: An in-depth benchmarking study. In Proceedings of the 2017 ACM international conference on management of data, pages 651–666.

Azaria, A., Hassidim, A., Kraus, S., Eshkol, A., Weintraub, O., and Netanely, I. (2013). Movie recommender system for profit maximization. In Proceedings of the 7th ACM conference on Recommender systems, pages 121–128.

Bass, F. M. (1969). A new product growth for model consumer durables. Management science, 15(5):215–227.

Bass, F. M., Krishnan, T. V., and Jain, D. C. (1994). Why the bass model fits without decision variables. Marketing science, 13(3):203–223.

Besbes, O., Gur, Y., and Zeevi, A. (2016). Optimization in online content recommendation services: Beyond click-through rates. Manufacturing & Service Operations Management, 18(1):15–33.

Bretthauer, K. M. and Shetty, B. (1995). The nonlinear resource allocation problem. Operations research, 43(4):670–683.

Bretthauer, K. M. and Shetty, B. (2002). The nonlinear knapsack problem–algorithms and applications. European Journal of Operational Research, 138(3):459–472.

Chen, N. and Chen, Y.-J. (2021). Duopoly competition with network effects in discrete choice models. Operations Research, 69(2):545–559.

Chen, Y. and Shi, C. (2019). Joint pricing and inventory management with strategic customers. Operations Research, 67(6):1610–1627.

Covington, P., Adams, J., and Sargin, E. (2016). Deep neural networks for youtube recommendations. In Proceedings of the 10th ACM conference on recommender systems, pages 191–198.

Davidson, J., Liebald, B., Liu, J., Nandy, P., Van Vleet, T., Gargi, U., Gupta, S., He, Y., Lambert, M., Livingston, B., et al. (2010). The youtube video recommendation system. In Proceedings of the fourth ACM conference on Recommender systems, pages 293–296.

Du, C., Cooper, W. L., and Wang, Z. (2016). Optimal pricing for a multinomial logit choice model with network effects. Operations Research, 64(2):441–455.

Easingwood, C. J., Mahajan, V., and Muller, E. (1983). A nonuniform influence innovation diffusion model of new product acceptance. Marketing Science, 2(3):273–295.

Feng, J., Bhargava, H. K., and Pennock, D. M. (2007). Implementing sponsored search in web search engines: Computational evaluation of alternative mechanisms. INFORMS Journal on Computing, 19(1):137–148.

FOX32 (2020). Missing child alert canceled after 2 chipley girls found safe; mom in custody. `https://www.fox32chicago.com/news/missing-child-alert-canceled-after-2-chipley-girls-found-safe-mom-in-custody`. Accessed: 2022-03-16.

Goldenberg, J., Libai, B., and Muller, E. (2001). Talk of the network: A complex systems look at the underlying process of word-of-mouth. Marketing letters, 12(3):211–223.

Golrezaei, N., Nazerzadeh, H., and Randhawa, R. (2020). Dynamic pricing for heterogeneous time-sensitive customers. Manufacturing & Service Operations Management, 22(3):562–581.

Granovetter, M. (1978). Threshold models of collective behavior. American journal of sociology, 83(6):1420–1443.

Hochbaum, D. S. (1995). A nonlinear knapsack problem. Operations Research Letters, 17(3):103–110.

Horsky, D. and Simon, L. S. (1983). Advertising and the diffusion of new products. Marketing Science, 2(1):1–17.

Hu, M., Milner, J., and Wu, J. (2016). Liking and following and the newsvendor: Operations and marketing policies under social influence. Management Science, 62(3):867–879.

Jiang, Z. and Jain, D. C. (2012). A generalized norton–bass model for multigeneration diffusion. Management Science, 58(10):1887–1897.

Kempe, D., Kleinberg, J., and Tardos, É. (2003). Maximizing the spread of influence through a social network. In Proceedings of the ninth ACM SIGKDD international conference on Knowledge discovery and data mining, pages 137–146.

Kiesling, E., Günther, M., Stummer, C., and Wakolbinger, L. M. (2012). Agent-based simulation of innovation diffusion: a review. Central European Journal of Operations Research, 20(2):183–230.

Kitts, B., Freed, D., and Vrieze, M. (2000). Cross-sell: a fast promotion-tunable customer-item recommendation method based on conditionally independent probabilities. In Proceedings of the sixth ACM SIGKDD international conference on Knowledge discovery and data mining, pages 437–446.

Li, D. and Sun, X. (2006). Nonlinear integer programming, volume 84. Springer Science & Business Media.

Li, Y., Fan, J., Wang, Y., and Tan, K.-L. (2018). Influence maximization on social graphs: A survey. IEEE Transactions on Knowledge and Data Engineering, 30(10):1852–1872.

Liu, J., Dolan, P., and Pedersen, E. R. (2010). Personalized news recommendation based on click behavior. In Proceedings of the 15th international conference on Intelligent user interfaces, pages 31–40.

Liu, X. and Aberer, K. (2013). Soco: a social network aided context-aware recommender system. In Proceedings of the 22nd international conference on World Wide Web, pages 781–802.

Lu, W., Chen, S., Li, K., and Lakshmanan, L. V. (2014). Show me the money: dynamic recommendations for revenue maximization. Proceedings of the VLDB Endowment, 7(14):1785–1796.

Ma, T., Zhou, J., Tang, M., Tian, Y., Al-Dhelaan, A., Al-Rodhaan, M., and Lee, S. (2015). Social network and tag sources based augmenting collaborative recommender system. IEICE transactions on Information and Systems, 98(4):902–910.

Nemhauser, G. L., Wolsey, L. A., and Fisher, M. L. (1978). An analysis of approximations for maximizing submodular set functions—i. Mathematical programming, 14(1):265–294.

Nielsen, S. S. and Zenios, S. A. (1992). Massively parallel algorithms for singly constrained convex programs. ORSA Journal on Computing, 4(2):166–181.

Niu, S.-C. (2002). A stochastic formulation of the bass model of new-product diffusion. Mathematical problems in Engineering, 8(3):249–263.

Norton, J. A. and Bass, F. M. (1987). A diffusion theory model of adoption and substitution for successive generations of high-technology products. Management science, 33(9):1069–1086.

Nosrat, F., Cooper, W. L., and Wang, Z. (2021). Pricing for a product with network effects and mixed logit demand. Naval Research Logistics (NRL), 68(2):159–182.

Resnick, P., Iacovou, N., Suchak, M., Bergstrom, P., and Riedl, J. (1994). Grouplens: an open architecture for collaborative filtering of netnews. In Proceedings of the 1994 ACM conference on Computer supported cooperative work, pages 175–186.

Satoh, D. (2001). A discrete bass model and its parameter estimation. Journal of the Operations Research Society of Japan, 44(1):1–18.

Schelling, T. C. (2006). Micromotives and macrobehavior. WW Norton & Company.

Schmittlein, D. C. and Mahajan, V. (1982). Maximum likelihood estimation for an innovation diffusion model of new product acceptance. Marketing science, 1(1):57–78.

Snyder, L. V. and Shen, Z.-J. M. (2019). Fundamentals of supply chain theory. John Wiley & Sons.

Srinivasan, V. and Mason, C. H. (1986). Nonlinear least squares estimation of new product diffusion models. Marketing science, 5(2):169–178.

Statista (2021). Youtube average video length by category 2018. `https://www.statista.com/statistics/1026923/youtube-video-category-average-length/`. Accessed: 2022-03-11.

Su, X. and Khoshgoftaar, T. M. (2009). A survey of collaborative filtering techniques. Advances in artificial intelligence, 2009.

Sultan, F., Farley, J. U., and Lehmann, D. R. (1990). A meta-analysis of applications of diffusion models. Journal of marketing research, 27(1):70–77.

Teng, J. T., Grover, V., and Guttler, W. (2002). Information technology innovations: general diffusion patterns and its relationships to innovation characteristics. IEEE transactions on engineering management, 49(1):13–27.

TikTok (2021). squidgame hashtag videos on tiktok. `https://www.tiktok.com/tag/squidgame`. Accessed: 2022-03-16.

Vahabi, H., Koutsopoulos, I., Gullo, F., and Halkidi, M. (2015). Difrec: A social-diffusion-aware recommender system. In Proceedings of the 24th ACM International on Conference on Information and Knowledge Management, pages 1481–1490.

Wang, R. and Wang, Z. (2017). Consumer choice models with endogenous network effects. Management Science, 63(11):3944–3960.

YouTube (2021). Youtube for press. `https://blog.youtube/press/`. Accessed: 2022-03-11.

Zhang, H. and Vorobeychik, Y. (2019). Empirically grounded agent-based models of innovation diffusion: a critical review. Artificial Intelligence Review, pages 1–35.

Appendix A: Diffusion model with discounted adopters

A.1. OBM with discounted adopters

In BDM, it is assumed that the imitative effect is proportional to the number of adopters. However, the network effect is usually time-sensitive and the incentive for adopters to share this information also decays with time. This phenomenon is more significant in the online platform as an explosive number of information are competing for attention. Therefore, we define the discounted adopters as $\tilde{A}_t = \sum_{\tau=1}^{t} \gamma_\tau a_\tau$ where $0 \le \gamma_i \le 1$ are discount factors. A common practice of the discounted adopters is exponentially smoothed decay where $\tilde{A}_t = \sum_{\tau=1}^{t} \gamma^{t-\tau} a_\tau$.

The formulation of OBM with discounted adopter can be written as

$$a_t = p(m - A_{t-1})x_t + \frac{q}{m}\tilde{A}_{t-1}(m - A_{t-1}) \tag{9}$$

A.2. CGP problem with Discounted Adopters

When the discounted adopters are used in the diffusion process as (9), we can similarly formulate the CGP problem.

For some extreme cases, when $\gamma_\tau = 1$ for all $\tau = 0, 1, \ldots, T$, it is just the case we formulate before without discount; when $\gamma_\tau = 0$ for all $\tau = 0, 1, \ldots, T$, there is no imitative effect. For other general cases, we claim that the Adaptive Greedy Algorithm can still be applied and the same approximation rate can be achieved.

As the submodularity of $U(V)$ relies on the problem structure of the CGP problem, replacing the imitative effect with the discounted adopters $A_{v,t}$ will lead to a different implicit reward function $R(\boldsymbol{x})$. However, the new reward function is still monotone and concave which builds the foundation of the submodularity and Adaptive Greedy Algorithm. As the discounted adopter $A_{v,t}$ is designed to be no larger than the original $A_{v,t}$, we can still have the inequalities (11b) and (12b) hold by $\tilde{A}_{v,t} \le A_{v,t} \le m$. As a result, all the following properties hold. Therefore, CGP problem with discounted adopters can use the same algorithms as shown in previous sections.

While having the difficulty and time complexity almost the same, the main difference in considering the discounted adopters is that more information is needed for the calculation. To keep track of the adoption sequence, it is not sufficient to only know $A_{v,0}$ before the CGP problem, but the entire adoption history is needed. The exponential smoothed decay is one of the simplest discount method since it include only one factor. It also does not need to know the entire adoption history as the discounted adopters can be recursively written as $\tilde{A}_{v,t} = \gamma \tilde{A}_{v,t-1} + a_{v,t-1}$. Thus, it is used in our following estimation analysis and numerical experiments.

Appendix B: Proofs

B.1. Proofs in Section 4

Proof of Theorem 1: Consider a special case of our problem when $L = 2$ and $A_{v,0} = 0$ for all content $v \in \mathcal{V}$. We can reformulate the problem as

$$\underset{\boldsymbol{x}, V}{\text{maximize}} \quad \sum_{v \in \mathcal{V}} -(1+q_v)p_v^2 m x_v^2 + (2+q_v)p_v m x_v$$

$$\text{subject to} \quad |V| \leq K,$$
$$\sum_{v \in \mathcal{V}} x_v = 1,$$
$$0 \leq x_v \leq \mathbb{1}\{v \in V\}, \forall v \in \mathcal{V}.$$

Let $\alpha_v = (1+q_v)p_v^2 m$ and $\beta_v = (2+q_v)p_v m$. Let s_i be some arbitrary numbers such that $s_i \in [0,1]$. We construct the quadratic objective for all content v that satisfies the following equations

$$\begin{cases} -2\alpha_v s_v + \beta_v & = C \\ \alpha_v s_v^2 & = D \end{cases} \tag{10}$$

where C and D are two fixed constants. Let $R(\boldsymbol{x}) = \sum_{v \in \mathcal{V}} -\alpha_v x_v^2 + \beta_v x_v$, we claim that

$$R(\boldsymbol{x}^*) \geq C + DK \Longleftrightarrow \text{ there exists } V \subseteq \mathcal{V} \text{ with } |V| = K \text{ and } \sum_{v \in V} s_v = 1$$

For the objective value we have

$$\begin{aligned} R(\boldsymbol{x}) &= \sum_{v \in \mathcal{V}} -\alpha_v x_v^2 + \beta_v x_v \\ &\leq \sum_{v \in \mathcal{V}} \left[(-2\alpha_v s_v + \beta_v)(x_v - s_v) - a_v s_v^2 + \beta_v s_v\right] \cdot \mathbb{1}\{v \in V\} \\ &= \sum_{v \in \mathcal{V}} (-2\alpha_v s_v + \beta_v) x_v + \alpha_v s_v^2 \cdot \mathbb{1}\{v \in V\} \\ &= \sum_{v \in \mathcal{V}} C x_i + D \cdot \mathbb{1}\{v \in V\} \\ &\leq C + DK \end{aligned}$$

where the first inequality follows from the concavity of $R(\cdot)$ and the last inequality follows since V contains at most k values of v. Equality holds if and only if $x_v = s_v$ for all $v \in V$. In other words, equality holds if and only if $\sum_{v: v \in V} s_v = 1$.

The claim above allows to reduce SUBSET-SUM to our problem as follows. Let positive integers $c_1, \ldots c_n$ and C form an instance of SUBSET-SUM. Without loss of generality, we can assume that $c_i \leq C$ for all $i \in \{1, 2, \ldots, n\}$. Let $s_i = c_i / C$. There exists a subset $I \subseteq \{1, \ldots, n\}$ such that $\sum_{i \in I} s_i = 1$ if and only if the objective value $R(\boldsymbol{x}^*)$ is at least $C + DK$ for some $k \in \{1, \ldots, n\}$.

For the rigour of proof, we then show that constants C and D exists. Suppose we normalize C and D with market size m. Plug p_v and q_v into (10), we get

$$p_v \left(1 + \frac{D}{p_v^2 s_v^2} - 2 s_v \frac{D}{p_v^2 s_v^2}\right) = C \Longrightarrow s_v^2 p_v^2 - C s_v^2 p_v + (1 - 2s_v) D = 0$$

When $C^2 \geq \frac{4(1-2s_v)D}{s_v^2}$ for all s_v, we can have $p_v = \frac{C}{2} - \sqrt{\frac{C^2}{4} - \frac{(1-2s_v)D}{s_v^2}}$ and $0 \leq p_v \leq 1$ holds. $q_v = \frac{D}{s_v^2 p_v^2} - 1$ and $0 \leq q_v \leq 1$ also holds. $\square$

Proof of Theorem 2: As $R(\boldsymbol{x})$ is the addition of $R_v(x_v)$, it suffices to show that $R_v(x_v)$ is strictly increasing and strictly concave. Analogy to $A_{v,L}$, $A_{v,t}$ for all $t = 1, 2, \cdots, L-1$ are also functions of x_v. We will show that all these functions are monotone and concave with regard to x_v.

We first show monotonicity by induction.

When $t=0$, $A_{v,1}=A_{v,0}+p_v(m-A_{v,0})x_v+\frac{q_v}{m}(m-A_{v,0})A_{v,0}$. Since $A_{v,0}$ is a constant, we have

$$\frac{dA_{v,1}}{dx_v}=p_v(m-A_{v,0})\geq 0$$

When $t>0$, we have

$$\begin{aligned}\frac{dA_{v,t}}{dx_v}&=p_v(m-A_{v,t-1})+(1-p_vx_v-2\frac{q_v}{m}A_{v,t-1}+q_v)\frac{dA_{v,t-1}}{dx_v} &\text{(11a)}\\&>(1-p_v-q_v)\frac{dA_{v,t-1}}{dx_v} &\text{(11b)}\\&\geq 0 &\text{(11c)}\end{aligned}$$

(11b) follows since $\frac{dA_{v,t-1}}{dx_v}\geq 0$ and by definition the feasible region of x_v is $0\leq x_v\leq 1$, $A_{v,t-1}<m$. (11c) follows since by definition $p_v+q_v\leq 1$.

Similarly, the concavity can also be shown by induction.

When $t=0$,

$$\frac{d^2A_{v,1}}{dx_v^2}=0\leq 0$$

When $t>0$, we have

$$\begin{aligned}\frac{d^2A_{v,t}}{dx_v^2}&=(-p_v-\frac{q_v}{m}\frac{dA_{v,t-1}}{dx_v})\frac{dA_{v,t-1}}{dx_v}+(1-p_vx_v-2\frac{q_v}{m}A_{v,t-1}+q_v)\frac{d^2A_{v,t-1}}{dx_v^2} &\text{(12a)}\\&<(-p_v-\frac{q_v}{m}\frac{dA_{v,t-1}}{dx_v})\frac{dA_{v,t-1}}{dx_v}+(1-p_v-q_v)\frac{d^2A_{v,t-1}}{dx_v^2} &\text{(12b)}\\&\leq 0 &\text{(12c)}\end{aligned}$$

(12b) follows since $\frac{d^2A_{v,t-1}}{dx_v^2}\leq 0$ and by definition the feasible region of x_v is $0\leq x_v\leq 1$, $A_{v,t}$ is no larger than m. (12c) follows since $\frac{dA_{v,t-1}}{dx_v}\geq 0$ and by definition $p_v+q_v\leq 1$. $\square$

Proof of Lemma 1: We will show the proof for a fixed instance $\mathcal{I}(V)$ in the following and thus ignore the parameter V in notation.

We proof by contradiction. Without loss of generality, let v_i be the content such that $\tilde{\eta}=\eta_{v_i}=g_{v_i}(x^*_{v_i})$. If $x^*_{v_i}=1$, then all other content $v\in V$ will have $x^*_v=0$ and the lemma holds trivially. Otherwise, assume there exists a content v_j such that $x^*_{v_j}>0$ and $\eta_{v_j}<\tilde{\eta}$. Consider a solution $\boldsymbol{x}$ that is given by

$$x^\epsilon_v=\begin{cases}x^*_v, & \text{when } v\notin\{v_i,v_j\}\\ x^*_{v_i}+\epsilon, & \text{when } v=v_i\\ x^*_{v_j}-\epsilon, & \text{when } v=v_j\end{cases}$$

where ϵ is a small positive number. Since $x^*_{v_i}<1$ and $x^*_{v_j}>0$, there exists $\epsilon>0$ that makes $\boldsymbol{x}^\epsilon$ a feasible solution to $\mathcal{I}(V)$. Consequently, for a feasible $\boldsymbol{x}$, we use the first order approximation to get

$$\begin{aligned}R(\boldsymbol{x}^\epsilon)-R(\boldsymbol{x}^*)&=\Big[R_{v_i}(x^*_{v_i})+g_{v_i}(x^*_{v_i})\epsilon+R_{v_j}(x^*_{v_j})-g_{v_j}(x^*_{v_j})\epsilon+\mathcal{O}(\epsilon^2)\Big]-\Big[R_{v_i}(x^*_{v_i})+R_{v_j}(x^*_{v_j})\Big]\\&=\Big[g_{v_i}(x^*_{v_i})-g_{v_j}(x^*_{v_j})\Big]\epsilon+\mathcal{O}(\epsilon^2)\end{aligned}$$

Since $g_{v_i}(x^*_{v_i})>g_{v_j}(x^*_{v_j})$, there exists $\epsilon>0$ that makes $R(\boldsymbol{x}^\epsilon)-R(\boldsymbol{x}^*)>0$ which contradicts with the optimality of $\boldsymbol{x}^*$. Thus, for any $x^*_{v_j}>0$, we have $\eta_{v_j}\geq\tilde{\eta}$.

By definition, $\eta_{v_j}\leq\tilde{\eta}$. We conclude the theorem holds. $\square$

Proof of Theorem 3: We show the proof of (i) and (ii) se.

Proof of (i): For a fixed $\mathcal{I}(V)$, let $\boldsymbol{x}^*$ and $\boldsymbol{x}'$ be two different optimal solutions. Define $\tilde{\eta}$ and $\tilde{\eta}'$ be the generalized marginal reward that is defined by $\boldsymbol{x}^*$ and $\boldsymbol{x}'$ according to (5), respectively.

If $\boldsymbol{x}^*$ and $\boldsymbol{x}'$ are both optimal, we can find $v_i, v_j \in V$ such that $x^*_{v_i} < x'_{v_i}$ and $x^*_{v_j} > x'_{v_j}$. As a result, the following two inequalities both hold by Lemma 1 but contradict with each other.

$$\tilde{\eta}(V) = \eta_{v_j}(V) < \eta'_{v_j}(V) \le \tilde{\eta}'(V)$$
$$\tilde{\eta}'(V) = \eta'_{v_i}(V) < \eta_{v_i}(V) \le \tilde{\eta}(V)$$

In conclusion, $\mathcal{I}(V)$ can only have a unique optimal solution $\boldsymbol{x}^*(V)$.

Proof of (ii): For a fixed $\mathcal{I}(V)$, we know the optimal solution satisfies $\sum_{v\in V} x^*_v = 1$. We have

$$\sum_{v\in \underline{V}_{\tilde{\eta}(V)}} 0 + \sum_{v\in \tilde{V}_{\tilde{\eta}(V)}} g_v^{-1}(\tilde{\eta}(V)) + \sum_{v\in \overline{V}_{\tilde{\eta}(V)}} 1 = 1$$

For all $\eta > \tilde{\eta}$ (resp. $\eta < \tilde{\eta}$), we will have $g^{-1}(\eta) \le g^{-1}(\tilde{\eta}(V))$ (resp. $g^{-1}(\eta) \ge g^{-1}(\tilde{\eta}(V))$) holds for all $v \in \tilde{V}$ and some of the inequalities are strict. Subsequently, $\sum_{v\in \underline{V}_\eta} 0 + \sum_{v\in \tilde{V}_\eta} g_v^{-1}(\eta) + \sum_{v\in \overline{V}_\eta} 1$ will not equal to 1. □

Proof of Lemma 2: We will show the proof for a pair of fixed instances $\mathcal{I}(V_1)$ and $\mathcal{I}(V_2)$ in the following.

Let V' be the set of content $v \in V_1$ that has different optimal solutions in $\mathcal{I}(V_1)$ and $\mathcal{I}(V_2)$, that is, $V' = \{v \in V_1 : x^*_v(V_1) \ne x^*_v(V_2)\}$. We only need to consider the case when $V' \ne \emptyset$ in the following proof.

Consider a solution $\boldsymbol{x}$ that is given by

$$x_v = \begin{cases} x^*_v(V_2), & \text{when } v \in V_1 \\ 0, & \text{when } v \notin V_1 \end{cases}$$

It is obvious that $\boldsymbol{x}$ is a feasible solution of $\mathcal{I}(V_1)$. By Theorem 2, we know that there exists $w \in V'$ such that $x^*_w(V_1) > x_w = x^*_w(V_2)$. $x^*_w(V_1) > x^*_w(V_2)$ directly implies that $\eta_w(V_1) < \eta_w(V_2)$, $x^*_w(V_1) > 0$. By Lemma 1, we have

$$\tilde{\eta}(V_1) = \eta_w(V_1) < \eta_w(V_2) \le \tilde{\eta}(V_2) \tag{13}$$

For all $v \in V'\backslash\{w\}$, if $x^*_v(V_2) = 0$, it is trivial that $x^*_v(V_2) < x^*_v(V_1)$. Otherwise, if $x^*_v(V_2) > 0$, we have $\tilde{\eta}(V_2) = \eta_v(V_2)$ from Lemma 1. We can thus have $\eta_v(V_1) < \eta_v(V_2)$ following (13), which further implies $x^*_v(V_1) > x^*_v(V_2)$.

$\tilde{\eta}(V_1) \le \tilde{\eta}(V_2)$ follows directly. If there exists $w \in V_2\backslash V_1$ such that $x^*_w(V_2) > 0$, at least one of $w \in V_1$ satisfies $x^*_w(V_1) \ne x^*_w(V_2)$. Consequently, inequality (13) also holds and $\tilde{\eta}(V_1) \le \tilde{\eta}(V_2)$. Otherwise, if for all $v \in V_2\backslash V_1$, $x^*_v(V_2) = 0$ holds, we can conclude that $\boldsymbol{x}^*(V_1) = \boldsymbol{x}^*(V_2)$ which leads to $\tilde{\eta}(V_1) = \tilde{\eta}(V_2)$.

In conclusion, $x^*_v(V_1) \ge x^*_v(V_2)$ and $\tilde{\eta}(V_1) \le \tilde{\eta}(V_2)$ for all $v \in V_1$ when $V_1 \subseteq V_2 \subseteq \mathcal{V}$. □

Proof of Theorem 4: It is trivial that $U(V_1) \le U(V_2)$ when $V_1 \subseteq V_2$, thus, $U(V)$ is monotone.

To show the submodularity, it suffices to show that

$$U(V_2 + \{w\}) - U(V_2) \le U(V_1 + \{w\}) - U(V_1)$$

where $V_1 \subseteq V_2$ and $w \in \mathcal{V}\backslash V_2$.

We consider a generalized version of parameterized problem (4), for a given set V, a content w not including in V with an upper bound s on promotion probability. The formulation can be written as

$$\begin{aligned} \underset{\boldsymbol{x}}{\text{maximize}} \quad & R(\boldsymbol{x}) \\ \text{subject to} \quad & \sum_{v \in V} x_v + x_w = 1, \\ & 0 \leq x_v \leq 1, \forall v \in V, \\ & 0 \leq x_w \leq s. \end{aligned}$$

With a little bit abuse of notation, in this case, we denote the instance as $\mathcal{I}(V,w,s)$. All the properties of the generalized marginal reward $\tilde{\eta}(V,w,s)$ and optimal solution $x^*(V,w,s)$ still hold.

Now that, consider a fixed pair of V and w when s changes. The optimal value $U(V,w,s)$ can be considered as a function of s. We decompose $U(V,w,s)$ as $U(V,w,s) = \sum_{v\in V} R_v(x_v^*(V,w,s)) + R_w(x_w^*(V,w,s))$. The negate of generalized marginal reward $-\tilde{\eta}(V,w,s)$ serve as the gradient of the reward function $\sum_{v\in V} R_v(x_v^*(V,w,s))$. We then have

$$\begin{aligned} & U(V,w,1) - U(V,w,0) \\ = & \sum_{v\in V} R_v(x_v^*(V,w,1)) - \sum_{v\in V} R_v(x^*(V,w,0)) + R_w(x^*(V,w,1)) - R_w(x_w^*(V,w,0)) \\ = & \int_{s=0}^{1} -\tilde{\eta}(V,w,s) ds + R_w(x_w^*(V,w,1)) \end{aligned}$$

Therefore,

$$\begin{aligned} & U(V_1 + \{w\}) - U(V_1) - [U(V_2 + \{w\}) - U(V_2)] \\ = & \int_{s=0}^{1} [\tilde{\eta}(V_2,w,s) - \tilde{\eta}(V_1,w,s)] \, ds + R_w(x_w^*(V_1,w,1)) - R_w(x_w^*(V_2,w,1)) \\ \geq & 0 \end{aligned}$$

where the inequality follows from Lemma 2.

In conclusion, we can the monotonicity and submodularity of $U(V)$. $\square$

B.2. Proofs in Section 5

Proof of Theorem 5: We use $p\lim$ to denote the probability limit.

(i) The case when samples increase with time. Suppose there are T observations which comes from the same content but at different time. To make the growing data set valid, we first propose three assumptions on observations. The observations are valid in the sense that: $\forall \epsilon > 0$ such that

a) $1 - x_t > \epsilon$, $\forall t$,

b) $A_t > \epsilon$, $\forall t$,

c) $\frac{A_t}{m} < 1 - \epsilon$, $\forall t$,

Assumption a) is reasonable since in reality, it is rarely that the platform promotes only one content. Assumption b) is reasonable since as long as there exists adopters, the imitative effect would become a positive number. Assumption c) is needed to study the asymptotic case when T tends to infinity. If $A_T = m$, then there will be only finite observations. Therefore, we assume m scales with T. As a result, $(1-x_t)z_{t,2} > \epsilon^4$.

As $\hat{q}^{\mathrm{D}} = q + \frac{\sum_{t=1}^{T}\left[(1-x_t)z_{t,2}\epsilon_t^{\mathrm{im}}\right]}{\sum_{t=1}^{T}\left[(1-x_t)z_{t,2}\right]^2}$, with valid observations, we have

$$p\lim|\hat{q}^{\mathrm{D}} - q| \le p\lim\left(\frac{1}{T}\sum_{t=1}^{T}(1-x_t)z_{t,2}\epsilon_t^{\mathrm{im}}\right)\cdot\epsilon$$

Let $S_T = \sum_{t=1}^{T}(1-x_t)z_{t,2}\epsilon_t^{\mathrm{im}}$. Since data is observed sequentially, we cannot directly apply the Weak Law of Large number to $\frac{S_T}{T}$. However, we can still show it converges to its mean $\mathbb{E}[(1-x)z_2\epsilon^{\mathrm{im}}]$.

We first calculate the mean $\mathbb{E}[(1-x)z_2\epsilon^{\mathrm{im}}]$. Since $z_{t,2}$ is only related to the number of adopters before t, the random noise ϵ^{im} is independent with $(1-x)z_2$. We have the mean

$$\mathbb{E}[(1-x)z_2\epsilon^{\mathrm{im}}] = \mathbb{E}\left[(1-x)z_2\right]\mathbb{E}\left[\epsilon^{\mathrm{im}}\right] = 0$$

The convergence in probability of $\frac{S_T}{T}$ is then shown as follows. By Chebyshev's inequality, we have

$$\mathbb{P}\left(\left|\frac{S_T}{T} - 0\right| > \xi\right) \le \frac{\mathrm{var}(\frac{S_T}{T})}{\xi^2} = \frac{\mathrm{var}(S_T)}{T^2\xi^2}$$

The variance can be decomposed as

$$\mathrm{var}(S_T) = \sum_{t=1}^{T}\sum_{\tau\neq t}\mathrm{cov}\left((1-x_t)z_{t,2}\epsilon_t^{\mathrm{im}}, (1-x_\tau)z_{\tau,2}\epsilon_\tau^{\mathrm{im}}\right) + \sum_{t=1}^{T}\mathrm{var}\left((1-x_t)z_{t,2}\epsilon_t^{\mathrm{im}}\right)$$

Without loss of generality, suppose $t < \tau$, we have the covariance term becomes

$$\begin{aligned}
&\mathrm{cov}\left((1-x_t)z_{t,2}\epsilon_t^{\mathrm{im}}, (1-x_\tau)z_{\tau,2}\epsilon_\tau^{\mathrm{im}}\right)\\
=&\mathbb{E}[(1-x_t)z_{t,2}\epsilon_t^{\mathrm{im}}(1-x_\tau)z_{\tau,2}\epsilon_\tau^{\mathrm{im}}] - \mathbb{E}[(1-x_t)z_{t,2}\epsilon_t^{\mathrm{im}}]\mathbb{E}[(1-x_\tau)z_{\tau,2}\epsilon_\tau^{\mathrm{im}}]\\
=&\mathbb{E}[\epsilon_\tau^{\mathrm{im}}]\mathbb{E}[(1-x_t)z_{t,2}\epsilon_t^{\mathrm{im}}(1-x_\tau)z_{\tau,2}] - 0\\
=&0
\end{aligned}$$

where the equalities follow since $\epsilon_\tau^{\mathrm{im}}$ is independent with all other terms.

The variance term becomes

$$\begin{aligned}
\mathrm{var}\left((1-x_t)z_{t,2}\epsilon_t^{\mathrm{im}}\right) &= \mathbb{E}[(1-x)^2z_2^2{\epsilon^{\mathrm{im}}}^2] - \mathbb{E}[(1-x)z_2\epsilon^{\mathrm{im}}]^2\\
&= \mathbb{E}[{\epsilon^{\mathrm{im}}}^2]\mathbb{E}[(1-x)^2z_2^2] - 0\\
&\le (1-\mu_x)^2m^4\sigma^2
\end{aligned}$$

where the expectation of $z_{t,2}^2$ is bounded since the number of adopters A will be no larger than market size m. Then, we have $\mathrm{var}(S_T) \le T(1-\mu_x)^2m^4\sigma^2$, and $\mathbb{P}\left(\left|\frac{S_T}{T} - 0\right| > \xi\right) \le \frac{(1-\mu_x)^2m^4\sigma^2}{T\xi^2}$. When T goes to infinity, $\frac{S_T}{T}$ converges to 0.

Therefore, we have $p\lim\hat{q}^{\mathrm{D}} = q$.

Similarly, for $\hat{p}^{\mathrm{D}} = p + \frac{\sum_{t=1}^{T}\left[z_{t,1}((q-\hat{q}^{\mathrm{D}})x_tz_{t,2}+\epsilon_t^{\mathrm{in}})\right]}{\sum_{t=1}^{T}z_{t,1}^2}$, we have

$$p\lim|\hat{p}^{\mathrm{D}} - p| \le p\lim\left(\frac{1}{T}\sum_{t=1}^{T}(q-\hat{q}^{\mathrm{D}})x_tz_{t,1}z_{t,2}\right)\epsilon + p\lim\left(\frac{1}{T}\sum_{t=1}^{T}z_{t,1}\epsilon_t^{\mathrm{in}}\right)\epsilon$$

We have the latter two terms of the above expression converge to 0. The first of these two terms converges to 0 since $p\lim|q-\hat{q}^{\mathrm{D}}| = 0$, and the second converges to 0 with the same reason as $\frac{S_T}{T}$.

As a result, we have $p\lim \hat{p}^{\mathrm{D}} = p$.

(ii) The case when samples increase with the number of content. Suppose there are N different content and for each content we make a fixed T number of observations.

The probability limit of $\hat{q}^{\mathrm{D}}$ can then be written as

$$p\lim \hat{q}^{\mathrm{D}} = q + p\lim\left(\frac{1}{\frac{1}{TN}\sum_{i=1}^{N}\sum_{t=1}^{T}\left[(1-x_{i,t})z_{i,t,2}\right]^2}\right)\cdot p\lim\left(\frac{1}{TN}\sum_{i=1}^{N}\sum_{t=1}^{T}(1-x_{i,\tau})z_{i,t,2}\epsilon_{i,t}^{\mathrm{im}}\right)$$

If we consider the sum of variables of the same content i as a random variable, we can follow the same procedure as (i) to derive $p\lim \hat{p}^{\mathrm{D}} = p$ and $p\lim \hat{q}^{\mathrm{D}} = q$. $\square$

Proof of Theorem 6: We consider two different estimation methods respectively.

(i) D-OLS estimation.

First, we consider the limiting distribution of $\frac{1}{\sqrt{NT}}(\hat{q}^{\mathrm{D}} - q)$.

$$\frac{1}{\sqrt{NT}}(\hat{q}^{\mathrm{D}} - q) = \frac{\frac{1}{\sqrt{NT}}\sum_{i=1}^{N}\sum_{t=1}^{T}[(1-x_{i,t})z_{i,t,2}\epsilon_{i,t}^{\mathrm{im}}]}{\frac{1}{NT}\sum_{i=1}^{N}\sum_{t=1}^{T}[(1-x_{i,t})z_{i,t,2}]^2}$$

We will show the denominator converges to $\mathbb{E}[(1-x)^2 z_2^2]$ in probability and the nominator converges to $\mathcal{N}(0, \mathbb{E}[(1-x)^2]^2\mathbb{E}[z_2^2]\sigma^2)$ in distribution.

For the denominator, we have the probability limit as

$$p\lim \frac{1}{NT}\sum_{i=1}^{N}\sum_{t=1}^{T}[(1-x_{i,t})z_{i,t,2}]^2 = \mathbb{E}\left[\frac{1}{T}\sum_{t=1}^{T}[(1-x_t)z_{t,2}]^2\right] = \mathbb{E}\left[(1-x)^2 z_2^2\right] = \mathbb{E}\left[(1-x)^2\right]\mathbb{E}\left[z_2^2\right]$$

For the nominator, consider the scaled sum $\frac{1}{\sqrt{T}}\sum_{t=1}^{T}[(1-x_t)z_{t,2}\epsilon_t^{\mathrm{im}}]$ as a random variable, we have

$$\mathbb{E}\left[\frac{1}{\sqrt{T}}\sum_{t=1}^{t}[(1-x_t)z_{t,2}\epsilon_t^{\mathrm{im}}]\right] = \sqrt{T}\mathbb{E}\left[(1-x)z_2\epsilon^{\mathrm{im}}\right] = \sqrt{T}\mathbb{E}\left[(1-x)z_2\right]\mathbb{E}\left[\epsilon^{\mathrm{im}}\right] = 0$$

and

$$\begin{aligned}
&\mathrm{var}\left(\frac{1}{\sqrt{T}}\sum_{t=1}^{T}[(1-x_t)z_{t,2}\epsilon_t^{\mathrm{im}}]\right)\\
=&\mathrm{var}\left((1-x)z_2\epsilon^{\mathrm{im}}\right) + \frac{1}{T}\sum_{t=1}^{T}\sum_{\tau\neq t}\mathrm{cov}\left((1-x_t)z_{t,2}\epsilon_t^{\mathrm{im}}, (1-x)z_{\tau,2}\epsilon_\tau^{\mathrm{im}}\right)\\
=&\mathbb{E}\left[(1-x)^2 z_2^2 {\epsilon^{\mathrm{im}}}^2\right] = \mathbb{E}\left[(1-x)^2 z_2^2\right]\mathbb{E}\left[{\epsilon^{\mathrm{im}}}^2\right]\\
=&\mathbb{E}\left[(1-x)^2 z_2^2\right]\mathbb{E}[(1-x)^2]\sigma^2
\end{aligned}$$

By Central Limit Theorem (CLT), we have

$$\frac{1}{\sqrt{NT}}\sum_{i=1}^{N}\sum_{t=1}^{T}[(1-x_{i,t})z_{i,t,2}\epsilon_{i,t}^{\mathrm{im}}] \xrightarrow{d} \mathcal{N}\left(0, \mathbb{E}\left[(1-x)^2\right]^2\mathbb{E}\left[z_2^2\right]\sigma^2\right)$$

Therefore, by Slutsky's theorem, the limiting distribution becomes

$$\frac{1}{\sqrt{NT}}(\hat{q}^{\mathrm{D}} - q) \xrightarrow{d} \mathcal{N}\left(0, \frac{1}{\mathbb{E}\left[z_2^2\right]}\sigma^2\right)$$

which implies the asymptotic variance of $\hat{q}^{\mathrm{D}}$ is $\frac{1}{\mathbb{E}[z_2^2]}\sigma^2$.

Next, we consider the limiting distribution $\frac{1}{\sqrt{NT}}(\hat{p}^{\mathrm{D}} - p)$.

$$\frac{1}{\sqrt{NT}}(\hat{p}^{\mathrm{D}}-p)=\frac{(q-\hat{q}^{\mathrm{D}})\frac{1}{\sqrt{NT}}\sum_{i=1}^{N}\sum_{t=1}^{T}x_{i,t}z_{i,t,1}z_{i,t,2}+\frac{1}{\sqrt{NT}}\sum_{i=1}^{N}\sum_{t=1}^{T}x_{i,t}z_{i,t,1}\epsilon_{i,t}^{\mathrm{in}}}{\frac{1}{NT}\sum_{i=1}^{N}\sum_{t=1}^{T}[x_{i,t}z_{i,t,1}]^2}$$

We will show the denominator converges to $\mathbb{E}[x^2z_1^2]$ in probability and the nominator converges to $\mathcal{N}(0,\mathbb{E}[x^2z_1^2]\sigma^2)$ in distribution.

For the denominator, we have the probability limit as

$$p\lim\frac{1}{NT}\sum_{i=1}^{N}\sum_{t=1}^{T}[x_{i,t}z_{i,t,1}]^2=\mathbb{E}\left[x^2z_1^2\right]$$

For the nominator, there are two terms and we consider them separately. Take the scaled sum $\frac{1}{\sqrt{T}}\sum_{t=1}^{T}x_tz_{t,1}z_{t,2}$ as a random variable, we have

$$\mathbb{E}\left[\frac{1}{\sqrt{T}}\sum_{t=1}^{T}x_tz_{t,1}z_{t,2}\right]=\sqrt{T}\mathbb{E}[xz_1z_2]$$

and suppose the variance of $\frac{1}{\sqrt{T}}\sum_{t=1}^{T}x_tz_{t,1}z_{t,2}$ is s, s is finite and upper bounded by

$$\mathrm{var}\left(\frac{1}{\sqrt{T}}\sum_{t=1}^{T}x_tz_{t,1}z_{t,2}\right)=\mathrm{var}\left(xz_1z_2\right)+\frac{1}{T}\sum_{t=1}^{T}\sum_{\tau\neq T}\mathrm{cov}\left(x_tz_{t,1}z_{t,2},x_\tau z_{\tau,1}z_{\tau,2}\right)\leq(T+1)\mu_x^2m^6$$

By CLT, we have

$$\frac{1}{\sqrt{NT}}\sum_{i=1}^{N}\sum_{t=1}^{T}[x_{i,t}z_{i,t,1}z_{i,t,2}]\xrightarrow{d}\mathcal{N}\left(\sqrt{T}\mathbb{E}[xz_1z_2],s\right)$$

From Theorem 5, $\hat{q}^{\mathrm{D}}-q\xrightarrow{p}0$. By Slutsky's theorem, we have

$$(q-\hat{q}^{\mathrm{D}})\frac{1}{\sqrt{NT}}\sum_{i=1}^{N}\sum_{t=1}^{T}x_{i,t}z_{i,t,1}z_{i,t,2}\xrightarrow{d}0\qquad\text{which implies}\qquad(q-\hat{q}^{\mathrm{D}})\frac{1}{\sqrt{NT}}\sum_{i=1}^{N}\sum_{t=1}^{T}x_{i,t}z_{i,t,1}z_{i,t,2}\xrightarrow{p}0$$

Consider the latter term, we take the scaled sum $\frac{1}{\sqrt{T}}\sum_{t=1}^{T}x_tz_{t,1}\epsilon_t^{\mathrm{in}}$ as a random variable. Similarly, we have $\mathbb{E}\left[\frac{1}{\sqrt{T}}\sum_{t=1}^{T}x_tz_{t,1}\epsilon_t^{\mathrm{in}}\right]=0$ and $\mathrm{var}\left(\frac{1}{\sqrt{T}}\sum_{t=1}^{T}x_tz_{t,1}\epsilon_t^{\mathrm{in}}\right)=\mathbb{E}\left[x^2z_1^2\right]\mathbb{E}[1-(1-x)^2]\sigma^2$. Thus, by CLT, we have $\frac{1}{\sqrt{NT}}\sum_{i=1}^{N}\sum_{t=1}^{T}x_tz_{t,1}\epsilon_t^{\mathrm{in}}\xrightarrow{d}\mathcal{N}(0,\mathbb{E}\left[x^2z_1^2\right]\mathbb{E}[1-(1-x)^2]\sigma^2)$.

Therefore, by Slutsky's theorem, the limiting distribution becomes

$$\frac{1}{\sqrt{NT}}(\hat{p}^{\mathrm{D}}-p)\xrightarrow{d}\mathcal{N}\left(0,\frac{\mathbb{E}[1-(1-x)^2]}{\mathbb{E}\left[x^2z_1^2\right]}\sigma^2\right)$$

which implies the asymptotic variance of $\hat{p}^{\mathrm{D}}$ is $\frac{\mathbb{E}[1-(1-x)^2]}{\mathbb{E}\left[x^2z_1^2\right]}\sigma^2$.

(ii) OLS estimation

For notation simplicity, we write the OLS formulation in matrix form. We define the following notation,

$$\boldsymbol{\beta}=\begin{pmatrix}p\\q\end{pmatrix},\qquad Z=\begin{pmatrix}x_1z_{1,1}&z_{1,1}z_{1,2}\\x_2z_{2,1}&z_{2,1}z_{1,2}\\\vdots&\vdots\\x_nz_{n,1}&z_{n,1}z_{n,2}\end{pmatrix},\qquad\boldsymbol{\epsilon}=\begin{pmatrix}\epsilon_1\\\epsilon_2\\\vdots\\\epsilon_n\end{pmatrix}$$

Consider the limiting distribution of $\frac{1}{\sqrt{NT}}(\hat{\boldsymbol{\beta}}-\boldsymbol{\beta})$, we have

$$\frac{1}{\sqrt{NT}}(\hat{\boldsymbol{\beta}}-\beta)=\left(\frac{1}{NT}(Z^TZ)\right)^{-1}\left(\frac{1}{\sqrt{NT}}Z^T\boldsymbol{\epsilon}\right)$$

For the first term, we have the probability limit as

$$Q = p\lim\left(\frac{1}{NT}(Z^T Z)\right)^{-1} = \begin{pmatrix} \mathbb{E}\left[\frac{1}{T}\sum_{t=1}^T x_t^2 z_{t,1}^2\right] & \mathbb{E}\left[\frac{1}{T}\sum_{t=1}^T x_t z_{t,1} z_{t,2}\right] \\ \mathbb{E}\left[\frac{1}{T}\sum_{t=1}^T x_t z_{t,1} z_{t,2}\right] & \mathbb{E}\left[\frac{1}{T}\sum_{t=1}^T z_{t,2}^2\right] \end{pmatrix}^{-1} = \begin{pmatrix} \mathbb{E}\left[x^2 z_1^2\right] & \mathbb{E}\left[x z_1 z_2\right] \\ \mathbb{E}\left[x z_1 z_2\right] & \mathbb{E}\left[z_2^2\right] \end{pmatrix}^{-1}$$

For the second term, we can apply multivariate CLT to get

$$\left(\frac{1}{\sqrt{NT}} Z^T \boldsymbol{\epsilon}\right) \xrightarrow{d} \mathcal{N}(\mathbf{0}, \Sigma)$$

where $\Sigma = \sigma^2 \begin{pmatrix} \mathbb{E}[x^2 z_1^2] & \mathbb{E}[x z_1 z_2] \\ \mathbb{E}[x z_1 z_2] & \mathbb{E}[z_2^2] \end{pmatrix}$.

By generalized Slutsky's theorem, we have $\frac{1}{\sqrt{NT}}(\hat{\boldsymbol{\beta}} - \boldsymbol{\beta}) \xrightarrow{d} \mathcal{N}(0, Q\Sigma Q^T)$. As we can find $Q\Sigma Q^T = \sigma^2 Q$, the asymptotic covariance matrix can be written as

$$\sigma^2 Q = \sigma^2 \begin{pmatrix} \frac{1}{\mathbb{E}\left[x^2 z_1^2\right]}\left(1 + \frac{\mathbb{E}[z_1 z_2]^2}{\mathbb{E}\left[z_1^2\right]\mathbb{E}\left[z_2^2\right] - \mathbb{E}[z_1 z_2]^2}\right) & -\frac{\mathbb{E}[z_1 z_2]}{\mathbb{E}\left[z_1^2\right]\mathbb{E}\left[z_2^2\right] - \mathbb{E}[z_1 z_2]^2} \\ -\frac{\mathbb{E}[z_1 z_2]}{\mathbb{E}\left[z_1^2\right]\mathbb{E}\left[z_2^2\right] - \mathbb{E}[z_1 z_2]^2} & \frac{1}{\mathbb{E}\left[z_2^2\right]}\left(1 + \frac{\mathbb{E}[z_1 z_2]^2}{\mathbb{E}\left[z_1^2\right]\mathbb{E}\left[z_2^2\right] - \mathbb{E}[z_1 z_2]^2}\right) \end{pmatrix}$$

Therefore, the asymptotic variances of $\hat{p}^{\text{OLS}}$ and $\hat{q}^{\text{OLS}}$ are $\frac{1}{\mathbb{E}\left[x^2 z_1^2\right]}\left(1 + \frac{\mathbb{E}[z_1 z_2]^2}{\mathbb{E}\left[z_1^2\right]\mathbb{E}\left[z_2^2\right] - \mathbb{E}[z_1 z_2]^2}\right)\sigma^2$ and $\frac{1}{\mathbb{E}\left[z_2^2\right]}\left(1 + \frac{\mathbb{E}[z_1 z_2]^2}{\mathbb{E}\left[z_1^2\right]\mathbb{E}\left[z_2^2\right] - \mathbb{E}[z_1 z_2]^2}\right)\sigma^2$, respectively. ☐

Appendix C: Numerical experiments

C.1. Data fitting of diffusion model

In general, there are two different approaches to evaluate the performance of the diffusion model and the estimation method. One is to consider the diffusion of a single piece of content. This approach is commonly used in the previous BDM literature. The performance is evaluated by conducting a look-ahead forecast. In particular, we estimate the parameters from the start of the specific diffusion to a certain time period, and then predict the number of new adopters in later periods. The other is to consider the diffusion of a category of content. In online content platforms, there is a great volume of content and a lot of content does not have sufficient adoption history. As a result, it is not applicable to estimate diffusion parameters separately for each piece of content. Instead, it is common to assume that the same diffusion parameters are shared by a category of content that has similar features. In particular, the parameters are estimated from the adoption history of part of content and the performance is evaluated on a holdout content set.

Both approaches are considered in this work. To show that BDM fails to capture the diffusion of online content, in Section 3.1, we consider a specific piece of content. When measuring the overall performance of different diffusion models and estimation methods, in Section 1.1 and Section 6.2, we consider a category of content that shares the same parameters.

C.1.1. Data fitting of BDM for a piece of content Parameters p, q, and m need to be estimated from historical data in order to fit BDM to real data. In our setting, m is known as the total number of users on the platform, thus, we only estimate p and q from data. To keep the consistency of the estimation method with Section 5, we use OLS on the following equation.

$$a_t = \left(p + \frac{q}{m} A_{t-1}\right)(m - A_{t-1}) = (m - A_{t-1}) \cdot p + \frac{A_{t-1}}{m}(m - A_{t-1}) \cdot q$$

where p and q have a linear relationship with the number of new adopters given the knowledge of previous adopters.

We observe $\{A_t\}_{t=0}^{T-1}$ and $\{a_t\}_{t=1}^{T}$ and change the length T of historical adoption data for estimation. All the fitted BDM curves show great deviation from the real adoption curves. Figure 1 shows the fitted Bass diffusion curves with parameters estimated based on the historical data from time $t=1$ to $t=50$.

C.1.2. Data fitting of OBM for a category of content To avoid overfitting issues, the content set of the same category is split into two parts: the training and testing sets. The parameters are estimated on the training set and evaluated on the testing set. Note that if a piece of content belongs to the training (resp. testing) set, the corresponding adoption data of all time periods are used for training (resp. testing).

The estimation of OBM requires the knowledge of $\{A_{v,t}\}_{t=0}^{T-1}$, $\{x_{v,t}\}_{t=1}^{T}$, and $\{a_{v,t}\}_{t=1}^{T}$ (or $\{a_{v,t}^{\text{in}}\}_{t=1}^{T}$, $\{a_{v,t}^{\text{im}}\}_{t=1}^{T}$) for all v in the training set. Note that we do not observe the promotion probability $x_{v,t}$ directly from the data. Instead, we obtain the number of users that have been targeted by platform promotion. During the estimation, we divide the number of targeted users by the entire market size m and consider this frequency to be the corresponding promotion probability.

After estimating the diffusion coefficients p and q via OLS (or D-OLS) method, we evaluate the performance on the testing set. The mean absolute percent error (MAPE) between the true value and predicted value of new adopters

$$\frac{1}{|\{(v,t)\}|}\sum_{(v,t)}\frac{|a_{v,t}-\hat{a}_{v,t}|}{a_{v,t}}$$

is used to measure the quality of the model.

C.1.3. Data fitting of OBM with discounted adopters To find the best discounted factor γ, we consider the average performance of all categories of content. For each category, we split the data set into three parts: the training, validation, and testing sets. For a given discounted factor γ, we fit our model on the training set and compute the measure of fit on the validation set. Afterward, we select the model with the γ associated with the best weighted average MAPE among all categories on the validation set. The weighted average MAPE takes the faction of data samples within each category as weight. Finally, we assess the performance of the model with the best discounted factor γ on the testing set.

For a given γ, we estimate p and q for each category via D-OLS estimation. We test the value of γ in the range of $(0,1]$ with the interval of 0.01. Figure 11 illustrates how the accuracy of prediction changes with discounted factor γ.

When $\gamma=0.26$, the weighted average MAPE attains the lowest point. We notice that the performance only changes slightly with small γ, so it is also reasonable to choose γ between 0 and 0.4. When $\gamma>0.8$, the MAPE increases rapidly as γ increases. It indicates that the incentive of diffusion decays fast for online content and the majority of imitative effect comes from the recent adopters. As the weighted average MAPE for $\gamma=1$ is over 60% more than the best value, the introduction of discount factor γ in OBM is necessary. From the diffusion perspective, the discounted effect shrinks the autocorrelation of the number of adopters in OBM as the imitative effect from a few time steps before can be ignored. This fact is indeed in favor of the accuracy of parameter estimation. From the promotion perspective, the platform's decision becomes much more important as the diffusion may not be able to cascade without promotion. In that sense, the promotion not only shortens the diffusion process but also triggers and leads the entire adoption procedure.

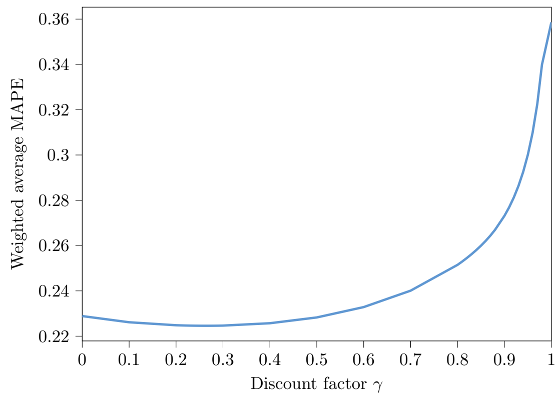

Figure 11 **MAPE between predicted adopters and the true values in validation set versus** γ

C.2. Numerical results

Table 3 **Numerical results for different candidate set size** K

K	$L=2$		$L=3$		$L=4$		$L=5$	
	gap (%)	CPU sec.	gap (%)	CPU sec.	gap (%)	CPU sec.	gap (%)	CPU sec.
10	1.11e-3	2.098	0.0726	8.175	1.970	15.358	3.352	20.233
20	9.63e-4	2.205	0.0666	9.426	1.857	23.609	2.819	33.425
30	9.63e-4	2.232	0.0529	9.784	1.673	27.429	2.793	43.962
40	9.63e-4	2.245	0.0301	10.105	1.405	32.605	2.647	51.250
50	9.63e-4	2.360	0.0179	10.342	1.241	36.220	2.117	61.581

Table 4 **Numerical results for different content size** $|\mathcal{V}|$

$\lvert\mathcal{V}\rvert$	$L=2$		$L=3$		$L=4$		$L=5$	
	gap (%)	CPU sec.	gap (%)	CPU sec.	gap (%)	CPU sec.	gap (%)	CPU sec.
200	8.387e-4	6.101	0.0322	19.447	1.755	56.864	3.285	116.831
400	4.435e-4	9.372	0.0681	38.013	2.170	101.242	3.167	231.439
600	2.342e-3	11.969	0.0781	47.851	2.104	142.515	3.265	348.737
800	2.024e-3	15.950	0.0729	60.563	2.140	187.972	3.306	406.708
1000	5.633e-3	18.960	0.0648	76.824	2.216	232.354	3.358	452.069